ornl

ORNL/TM-13684

OAK RIDGE
NATIONAL
LABORATORY

LOCKHEED MARTIN

INTERACTIONS OF ZIRCALOY CLADDING WITH GALLIUM: FINAL REPORT

D. F. Wilson
J. R. DiStefano
J. P. Strizak
J. F. King
E. T. Manneschmidt

MANAGED AND OPERATED BY
LOCKHEED MARTIN ENERGY RESEARCH CORPORATION
FOR THE UNITED STATES
DEPARTMENT OF ENERGY

ORNL-27 (3-96)

This report has been reproduced directly from the best available copy.

Available to DOE and DOE contractors from the Office of Scientific and Technical Information, P.O. Box 62, Oak Ridge, TN 37831; prices available from (423)576-8401.

Available to the public from the National Technical Information Service, U.S. Department of Commerce, 5285 Port Royal Rd., Springfield, VA 22161.

This report was prepared as an account of work sponsored by an agency of the United States Government. Neither the United States Government nor any agency thereof, nor any of their employees, makes any warranty, express or implied, or assumes any legal liability or responsibility for the accuracy, completeness, or usefulness of any information, apparatus, product, or process disclosed, or represents that its use would not infringe privately owned rights. Reference herein to any specific commercial product, process, or service by trade name, trademark, manufacturer, or otherwise, does not necessarily constitute or imply its endorsement, recommendation, or favoring by the United States Government or any agency thereof. The views and opinions of authors expressed herein do not necessarily state or reflect those of the United States Government or any agency thereof.

ORNL/TM-13684

Metals and Ceramics Division

INTERACTIONS OF ZIRCALOY CLADDING WITH GALLIUM: FINAL REPORT

D. F. Wilson
J. R. DiStefano
J. P. Strizak
J. F. King
E. T. Manneschmidt

Date Published: September 1998

Prepared for the
U.S. Department of Energy
Office of Fissile Materials Disposition
GA 01 02 01 4

Prepared by
OAK RIDGE NATIONAL LABORATORY
Oak Ridge, Tennessee 37831-6285
managed by
LOCKHEED MARTIN ENERGY RESEARCH CORP.
for the
U.S. DEPARTMENT OF ENERGY
under contract DE-AC05-96OR22464

CONTENTS

	Page
LIST OF FIGURES	v
LIST OF TABLES	vii
ACRONYMS	ix
ABSTRACT	xi
1. INTRODUCTION	1
2. OBJECTIVE	3
3. EXPERIMENTAL	5
4. RESULTS	11
4.1 PHASE I	11
4.1.1 Corrosion Tests	11
4.1.2 LME Tests	17
4.1.3 Corrosion-Mechanical Tests	22
4.2 PHASE II	24
4.2.1 Corrosion Tests	24
4.2.2 Corrosion-Mechanical Tests	30
4.2.2.1 Room-Temperature Mechanical Tests	30
4.2.2.2 High-Temperature Mechanical Tests	34
5. DISCUSSION	37
6. CONCLUSIONS	41
6.1 PHASE I	41
6.2 PHASE II	41
7. REFERENCES	43
APPENDIX	A-1

LIST OF FIGURES

Figure	Page
1. Test specimens. a, corrosion	6
2. Gallium containment system for LME tests	7
3. Out-of-reactor tests were not prototypic of LWR fuel system relative to density and gallium concentration	9
4. Intermetallic compounds formed between gallium and zirconium after 100 h at 400°C	11
5. Brittle intermetallic compounds formed between gallium and zirconium at 400°C	11
6. No attack of Zircaloy after 700 h at 30 or 100°C	12
7. Cross sections of Zircaloy tubes after corrosion testing with excess gallium (Ga) at 500°C for 200 h showing dimensional distortion	13
8. Corrosion testing with smaller amounts of gallium (Ga) at 500°C for 200 h	14
9. Porosity in Zr_xGa_y formed at 500°C in Zircaloy material	15
10. At 300°C, ICF decreases with decreasing time of exposure	16
11. ICF continues to decrease as the mass of gallium is decreased	17
12. LME tests showed no significant difference in strength for Zircaloy A at 30 and 100°C	19
13. LME tests showed no significant difference in ductility for Zircaloy A at 30 and 100°C	19
14. LME tests showed no significant difference in strength for Zircaloy B at 30 and 100°C	20
15. LME tests showed no significant difference in ductility for Zircaloy B at 30 and 100°C	20
16. LME test showed no change in strength for Zircaloy C at 30 and 100°C	21
17. LME tests showed no significant difference in ductility for Zircaloy C at 30 and 100°C	21
18. Ductile failure mode at 30 and 100°C with and without gallium	22
19. No change in strength observed after reaction with gallium for 30 h at 300°C	23

20. No significant change in ductility observed after exposure to gallium for 30 h at 300°C 23

21. Ductile fracture observed after 30 h at 300°C without and with gallium 24

22. Zircaloy reacts with oxides at 500°C to form zirconium oxide 25

23. No significant reaction of Zircaloy with Ga_2O_3 after 12 weeks at 300°C 26

24. Oxide layer present at 500°C for all ratios of Ga_2O_3 to cerium oxide 27

25. Zr_xGa_y identified below the zirconium oxide layer after exposure to 100% Ga_2O_3 at 700°C 29

26. No significant change in room-temperature strength for Zircaloy A after exposure to Ga_2O_3 in cerium oxide (6 weeks at 300 and 500°C) 31

27. Slight change in room-temperature ductility for Zircaloy A after exposure to Ga_2O_3 in cerium oxide (6 weeks at 300 and 500°C) 31

28. No significant change in room-temperature strength for Zircaloy B after exposure to Ga_2O_3 in cerium oxide (6 weeks at 300 and 500°C) 32

29. Slight change in room-temperature ductility for Zircaloy B after exposure to Ga_2O_3 in cerium oxide (6 weeks at 300 and 500°C) 32

30. No significant change in room-temperature strength for Zircaloy C after exposure to Ga_2O_3 in cerium oxide (6 weeks at 300 and 500°C) 33

31. Slight change in room-temperature ductility for Zircaloy C after exposure to Ga_2O_3 in cerium oxide (6 weeks at 300 and 500°C) 33

32. No significant changes in 300°C strength and ductility for Zircaloy A after exposure to Ga_2O_3 in cerium oxide (6 weeks at 300°C) 34

33. No significant changes in 500°C strength and ductility for Zircaloy A after exposure to Ga_2O_3 in cerium oxide (6 weeks at 500°C) 35

34. No significant changes in 300°C strength and ductility for Zircaloy C after exposure to Ga_2O_3 in cerium oxide (6 weeks at 300°C) 36

35. No significant changes in 500°C strength and ductility for Zircaloy C after exposure to Ga_2O_3 in cerium oxide (6 weeks at 500°C) 36

36. Phase stability diagram for oxides of interest 39

LIST OF TABLES

Table		Page
1.	Composition of alloys based on zirconium	5
2.	Vicker hardness (25 g load) for Zircaloys after 200 h at 500 °C with gallium	15
A.1	Supplemental compatibility tests of zirconium/Zircaloy with gallium or Ga_2O_3 in support of test design	A-1
A.2	Status of corrosion tests of Zircaloy with gallium metal	A-3
A.3	Status of corrosion tests of Zircaloy with Ga_2O_3	A-4
A.4	Status of mechanical tests of Zircaloy with gallium metal	A-4
A.5	Status of room-temperature, corrosion-mechanical tests of Zircaloy with Ga_2O_3	A-5
A.6	Status of high-temperature tensile, corrosion-mechanical tests of Zircaloy with Ga_2O_3	A-5

ACRONYMS

CERT	constant extension rate tensile
EBW	electron beam welding
IC	intermetallic compound
ICF	intermetallic compound formation
LANL	Los Alamos National Laboratory
LBW	laser beam welding
LME	liquid metal embrittlement
LWR	light-water reactor
MOX	mixed oxide
ORNL	Oak Ridge National Laboratory
WG	weapons grade
wt	weight

ABSTRACT

A program was conducted to evaluate the effect of gallium in mixed-oxide (MOX) fuel derived from weapons-grade (WG) plutonium on Zircaloy cladding performance. A four-phase experimental program was designed to evaluate the performance of prototypic Zircaloy cladding materials against (1) liquid gallium (Phase I), (2) various concentrations of Ga_2O_3 (Phase II), (3) centrally heated surrogate fuel pellets with expected levels of gallium (Phase III), and (4) centrally heated prototypic MOX fuel pellets (Phase IV). This report describes the results of tests for Phases I and II.

Three types of tests were performed: (1) corrosion, (2) liquid metal embrittlement, and (3) corrosion-mechanical. These tests were to determine corrosion mechanisms, thresholds for temperature and concentration of gallium that delineate behavioral regimes, and changes in the mechanical properties of Zircaloy.

Results have generally been favorable for the use of WG-MOX fuel. The MOX fuel cladding, Zircaloy, does react with gallium to form intermetallic compounds at ≥300°C; however, this reaction is limited by the mass of gallium and is therefore not expected to be significant with a low level (parts per million) of gallium in the MOX fuel. Although continued migration of gallium into the initially formed intermetallic compound can result in large stresses that may lead to distortion, this was shown to be extremely unlikely because of the low mass of gallium or gallium oxide present and expected clad temperatures below 400°C. Furthermore, no evidence for grain boundary penetration by gallium or liquid metal embrittlement was observed.

1. INTRODUCTION

The U.S. Department of Energy has established a dual-track approach to the disposition of plutonium arising from the dismantling of nuclear weapons. Both immobilization and reactor-based mixed-oxide (MOX) fuel technologies are being evaluated. The reactor-based MOX fuel option requires assessment of the potential impact of concentrations of gallium (on the order of 1 to 10 ppm), not present in conventional MOX fuel, on cladding material performance. Three previous reports[1-3] identified several compatibility issues relating to the presence of gallium in MOX fuel and its possible reaction with fuel cladding.

Gallium initially present in weapons-grade (WG) plutonium is largely removed during processing to produce MOX fuel. After blending the plutonium with uranium, only 1 to 10 ppm gallium is expected in the sintered MOX fuel. Gallium present as gallium oxide (Ga_2O_3) could be evolved as the suboxide (Ga_2O). Migration of the evolved Ga_2O and diffusion of gallium in the MOX matrix along thermal gradients could lead to locally higher concentrations of Ga_2O_3. Thus, while an extremely low concentration of gallium in MOX fuel almost ensures a lack of significant interaction of gallium with Zircaloy fuel cladding, there remains a small probability that corrosion effects will not be negligible.

A number of reaction routes are possible in this clad-WG-MOX fuel system, including:

$$\left.\begin{array}{c} Ga_XO \cdot PuO_2 \\ or \\ Ga_2O \\ or \\ Ga_2O_3 \end{array}\right\} + Zircaloy \rightarrow Ga \rightarrow \left\{\begin{array}{c} Surface\ alloying \\ or \\ Grain\ boundary\ penetration \\ or \\ Liquid\ metal\ embrittlement \end{array}\right. ,$$

and

$$Ga_2O_3 + ZrO_2 \rightarrow \left\{\begin{array}{c} No\ reaction \\ or \\ Mixed\ oxide + crack + Ga \rightarrow \end{array}\right. \left\{\begin{array}{c} Surface\ alloying \\ or \\ Grain\ boundary\ penetration \\ or \\ Liquid\ metal\ embrittlement \end{array}\right. .$$

General corrosion in the form of surface alloying resulting from formation of intermetallic compounds between Zircaloy and gallium should be mass limited and, therefore, superficial because of the expected low ratio of gallium to the surface area or volume of the Zircaloy cladding. Although the expected concentration of gallium is low and there is very limited solubility of gallium in zirconium, especially at temperatures below 700°C,[4] grain boundary penetration and liquid metal embrittlement (LME) are forms of localized corrosion that were also considered.

One fuel system damage mechanism, pellet clad interaction, has led to some failure of the Zircaloy cladding in light-water reactors (LWRs). This has been attributed to stresses in the cladding and one or more aggressive fission products. Stress corrosion cracking by iodine[5, 6] and LME by cadmium[7, 8] have been reported, and it is known that Zircaloy can be embrittled by some low-melting metals, (e.g., mercury).[9] LME is a form of environmentally induced embrittlement that can induce cracking or loss of ductility. LME requires wetting and a tensile stress, but it does not require corrosion penetration. Experimentally, it has been demonstrated that gallium can cause embrittlement of some alloys (e.g., aluminum) at low temperatures,[10, 11] but experiments relative to LME of zirconium by gallium have been limited and inconclusive.[12]

This report describes a series of tests designed to establish the effects of low levels of residual gallium in WG-MOX fuel on its compatibility with Zircaloy. In addition, to establish damage mechanisms it was important to understand types of cladding interactions and available safety margins with respect to gallium concentration.

2. OBJECTIVE

The overall objective of this task is to demonstrate the effects of small concentrations of gallium in MOX fuel on the performance of the fuel system in an LWR. Although possible mechanisms for gallium interaction with Zircaloy have been identified,[1-3] no significant data exist that demonstrate whether such reactions actually occur under LWR conditions and whether these reactions have any significant effects on cladding performance. In the planned program, a graded, experimental approach was designed to determine whether low levels of gallium would result in damage to the fuel clad. This approach was divided into four phases. In Phase I, laboratory tests were conducted on three prototypic Zircaloy cladding materials in liquid gallium. Three types of tests were used: (1) corrosion, (2) LME, and (3) corrosion-mechanical. Corrosion tests consisted of time–temperature exposures of Zircaloy to liquid gallium. LME tests consisted of slow strain rate, constant extension rate tensile (CERT) tests in gallium metal at low temperature (30 and 100°C). Corrosion-mechanical tests consisted of first exposing the Zircaloy to gallium metal and then conducting a tensile test to evaluate corrosion product effects. Although these Phase I tests conditions (much higher relative amount of gallium compared with that in a fuel rodlet) are not representative of WG-MOX, they provide limiting boundary conditions for mechanistic studies. The test matrices for Phase I are shown in the Appendix.

In Phase II, two of the previously mentioned types of tests, corrosion and corrosion-mechanical, were conducted with the three cladding materials in contact with Ga_2O_3. In each type of test, four concentrations of Ga_2O_3 in Ce_2O_3 (surrogate for plutonium dioxide) were evaluated: 100, 1, 0.2, and 0.1 weight (wt) %. Although these levels of Ga_2O_3 are all considerably higher than those possible in a sintered MOX pellet,[13] they can be used to determine the types of reactions that could occur, and, like Phase I tests, they represent a conservative evaluation of Ga_2O_3 effects in this screening test phase. The test matrices for Phase II are shown in the Appendix.

Phase III tests were designed to expose cladding material to centrally heated surrogate fuel pellets manufactured by Los Alamos National Laboratory (LANL). These sintered, annular pellets, U/Ce/Ga/O, contain less than 0.001 wt % gallium and have a density of more than 94%. The Texas A&M University Nuclear Science Center designed a nonpressurized test system for the centrally heated pellet tests. To simulate the thermal gradients across operating reactor pellets and to test for thermally driven gallium diffusion, a small diameter (~0.46-cm outside diameter) electric heater is inserted into the center of the surrogate pellets. The heater is designed to operate at a temperature of about 1000°C with a linear power of 15.7 kW/m. The experiment is configured to produce a nominal cladding-pellet interface temperature of 400°C. Six 10.2-cm

"rodlets" can be centrally heated and individually withdrawn for evaluation. Phase III will not be completed as part of this program. However, the heat transfer modeling results will be reported elsewhere.

Work related to the planned Phase IV was not implemented. If conducted, Phase IV tests would have been similar to Phase III tests, except that prototypic MOX fuel pellets would have been used.

3. EXPERIMENTAL

Prototypical LWR cladding materials evaluated included Zircaloy-2, Zircaloy-4, and Zirlo. Compositional ranges for these alloys are presented in Table 1.

Table 1. Composition of alloys based on zirconium (weight percent except where noted)

Alloy	Sn	Fe	Cr	Ni	Nb	O (ppm)
Zircaloy-2*	1.2–1.7	0.07– 0.2	0.05–0.15	0.03–0.08		1000–1400
Zircaloy-4*	1.2–1.7	0.18–0.24	0.07–0.13			1000–1400
Zirlo†	0.96–0.98	0.094–0.105	79–83 ppm		1.02–1.14	900–1200

*R. W. Cahn, P. Haasen, and E. J. Kramer, "Materials, Science, and Technology," Vol. 10b, p. 11, *Nuclear Materials*, Part 2, 1994.
†G. P. Sabol et al., "In-Reactor Corrosion Performance of Zirlo and Zircaloy-4," *Zirconium in the Nuclear Industry: Tenth International Symposium,* pp. 724–744 in *ASTM STP 1245,* ed. A. M. Garde and E. R. Bradley, American Society for Testing and Materials, Philadelphia, 1994.

Zircaloy tubing was machined into two different lengths, one for corrosion tests and another for LME or corrosion-mechanical tests, as shown in Fig. 1. End caps with and without threaded ends were machined from Zircaloy bar stock for tensile and corrosion tests, respectively. First, one end cap was welded to the specimen tube, a predetermined quantity of reactant was then added, and the other end cap was welded in place. Because of the reactive nature of the zirconium alloys with oxygen and nitrogen, all welding was performed in either high vacuum using the electron beam welding (EBW) process or in a high-purity, helium-purged welding chamber using the laser beam welding (LBW) process. The completed test specimens for corrosion tests were encapsulated in an evacuated quartz capsule for atmospheric protection during high-temperature exposure (Fig. 1). For mechanical testing above 100°C, a vacuum chamber with induction heating was used to preclude reaction of the zirconium alloys with ambient oxygen and nitrogen during testing. For the LME tests, the system shown in Fig. 2 was used to contain the liquid gallium after fracture of the specimen. The specimen was heated using copper coils containing glycol from a recirculating constant temperature bath.

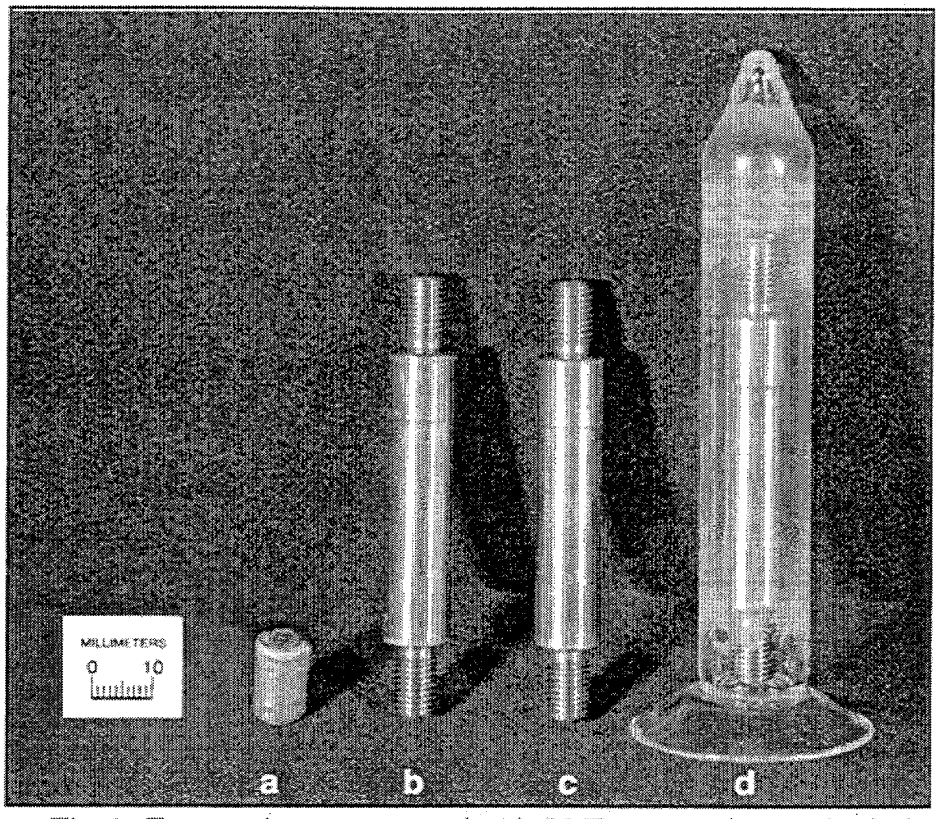

Fig. 1. Test specimens. a, corrosion; b, LME; c, corrosion-mechanical; d, encapsulated in quartz.

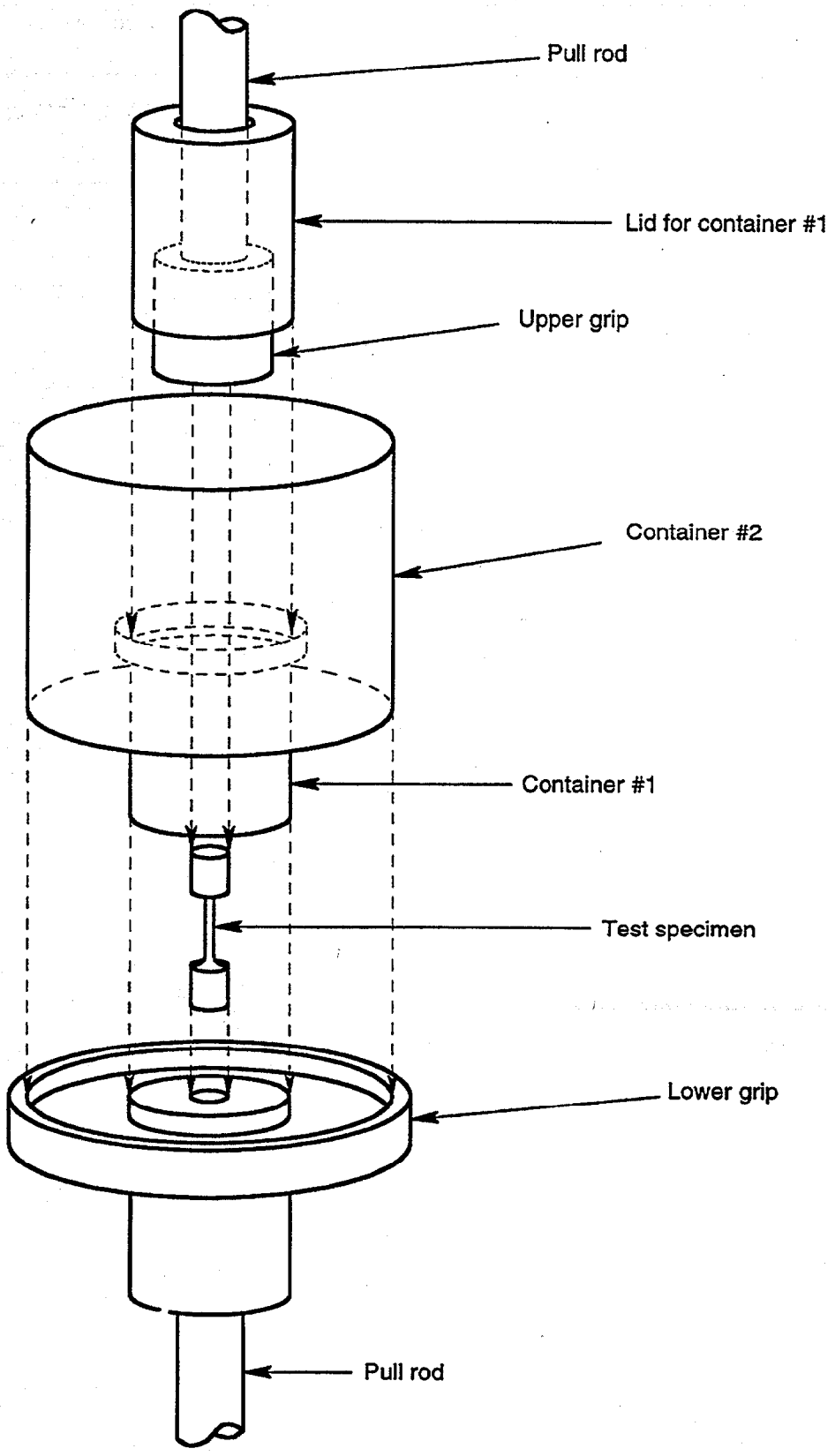

Fig. 2. Gallium containment system for LME tests.

In addition to preliminary tests that were performed at 400 and 600°C, corrosion tests in liquid gallium were conducted at three temperatures (30, 100, and 500°C) for two exposure times (200 and 700 h). Ga_2O_3 or surrogate gallium-containing oxide tests were also conducted at three temperatures (300, 500, and 700°C) for two exposure times (6 and 12 weeks). LME tests were conducted in liquid gallium at 30 and 100°C. Corrosion-mechanical tests in liquid gallium were conducted by first exposing the Zircaloy for 30 h at 300°C and then conducting a room-temperature tensile test. With Ga_2O_3, tensile tests were conducted at room temperature and at the corrosion test temperature after exposure for 6 weeks at 300 and 500°C. The temperature range brackets the normal, operating clad temperature of 374°C.

These tests were intended to characterize the types of gallium–cladding interaction that occur and determine how these interactions might affect cladding properties. Thus, the amount and distribution of gallium was significantly different than would occur in a fuel pin as indicated in Fig. 3. The MOX fuel consists of a high density, sintered pellet with a very small quantity (ppm level) of gallium. In contrast, Phase I and Phase II tests contain either 100% Ga (liquid or oxide) or low density powder mixtures of Ga_2O_3 with Ce_2O_3.

Posttest analyses of cross sections of the clad tubes included metallography, fractography, and chemical microprobe. In the case of the corrosion tests, evidence of wall thinning, grain boundary penetration, transgranular attack, and intermetallic compound formation (ICF), when present, were documented. For the mechanical tests (LME or corrosion-mechanical), the tensile strength and ductility of specimens tested in the presence of gallium or after exposure to gallium were compared with those tested in the absence of gallium.

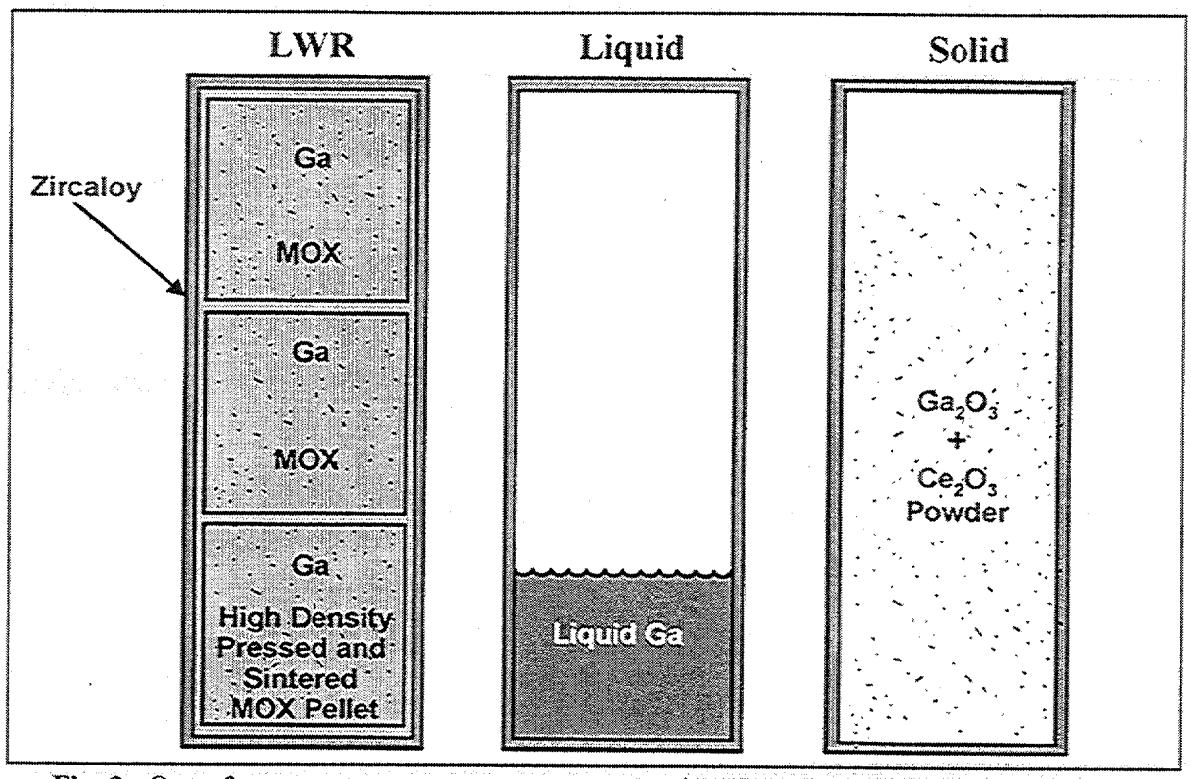

Fig. 3. Out-of-reactor tests were not prototypic of LWR fuel system relative to density and gallium concentration.

4. RESULTS

4.1 PHASE I

4.1.1 Corrosion Tests

In preliminary corrosion tests of zirconium by liquid gallium at 400°C and Zircaloy-2 (nonvendor-supplied) at 600°C, ICF was found as would be predicted from the gallium-zirconium phase diagram. As shown in Fig. 4, electron beam microprobe analysis identified several intermetallic compounds. No unreacted gallium remained in these tests. These intermetallic compounds are hard and brittle as shown in Fig. 5.

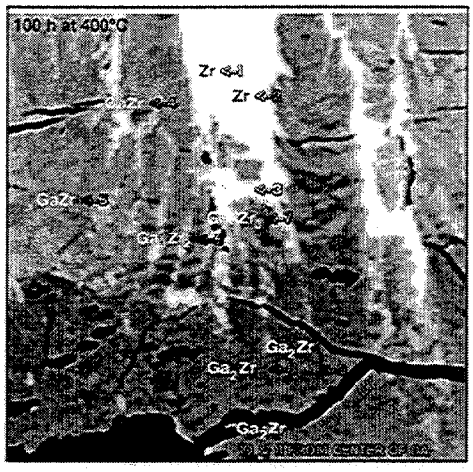

Fig. 4. Intermetallic compounds formed between gallium and zirconium after 100 h at 400°C.

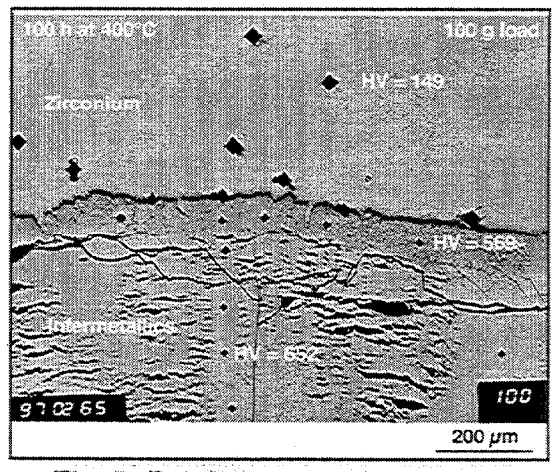

Fig. 5. Brittle intermetallic compounds formed between gallium and zirconium at 400°C.

After exposure to liquid gallium for 700 h at 30 and 100°C, none of the Zircaloy materials showed evidence of significant interaction as indicated by the typical results shown in Fig. 6. At 500°C, all of the gallium reacted with Zircaloy to form intermetallic compounds (ICs) of the type Zr_xGa_y after 200 or 700 h. Dimensional distortion of some Zircaloy capsules was observed as a result of exposure at 500°C (Fig. 7).

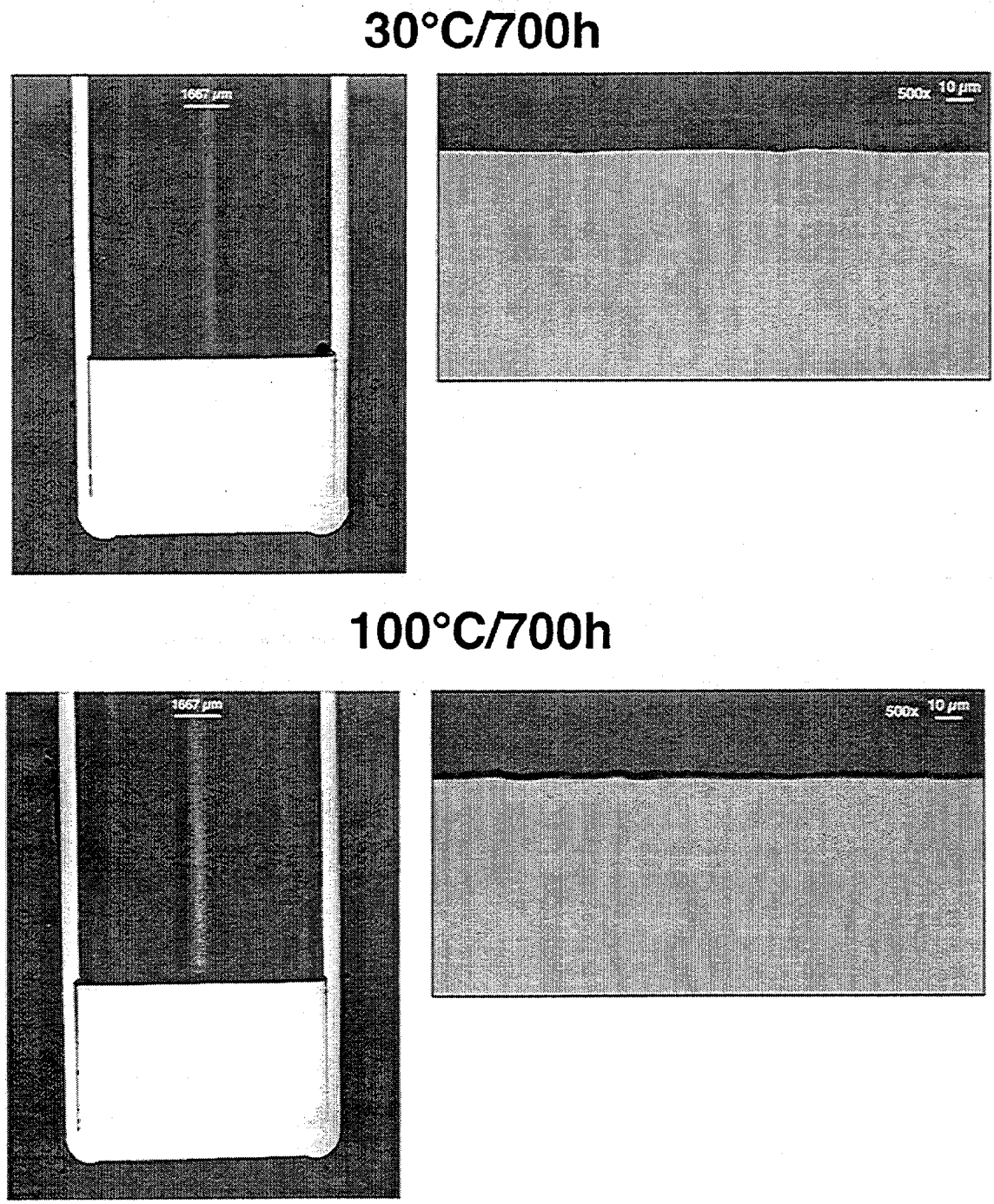

Fig. 6. No attack of Zircaloy after 700 h at 30 or 100°C.

Subsequent investigation revealed that the amount of distortion was not related to the end-cap geometry or the internal gas pressure [as determined by whether EBW or LBW (Fig. 7) was used]. However, distortion was a function of the amount of gallium initially in the capsule

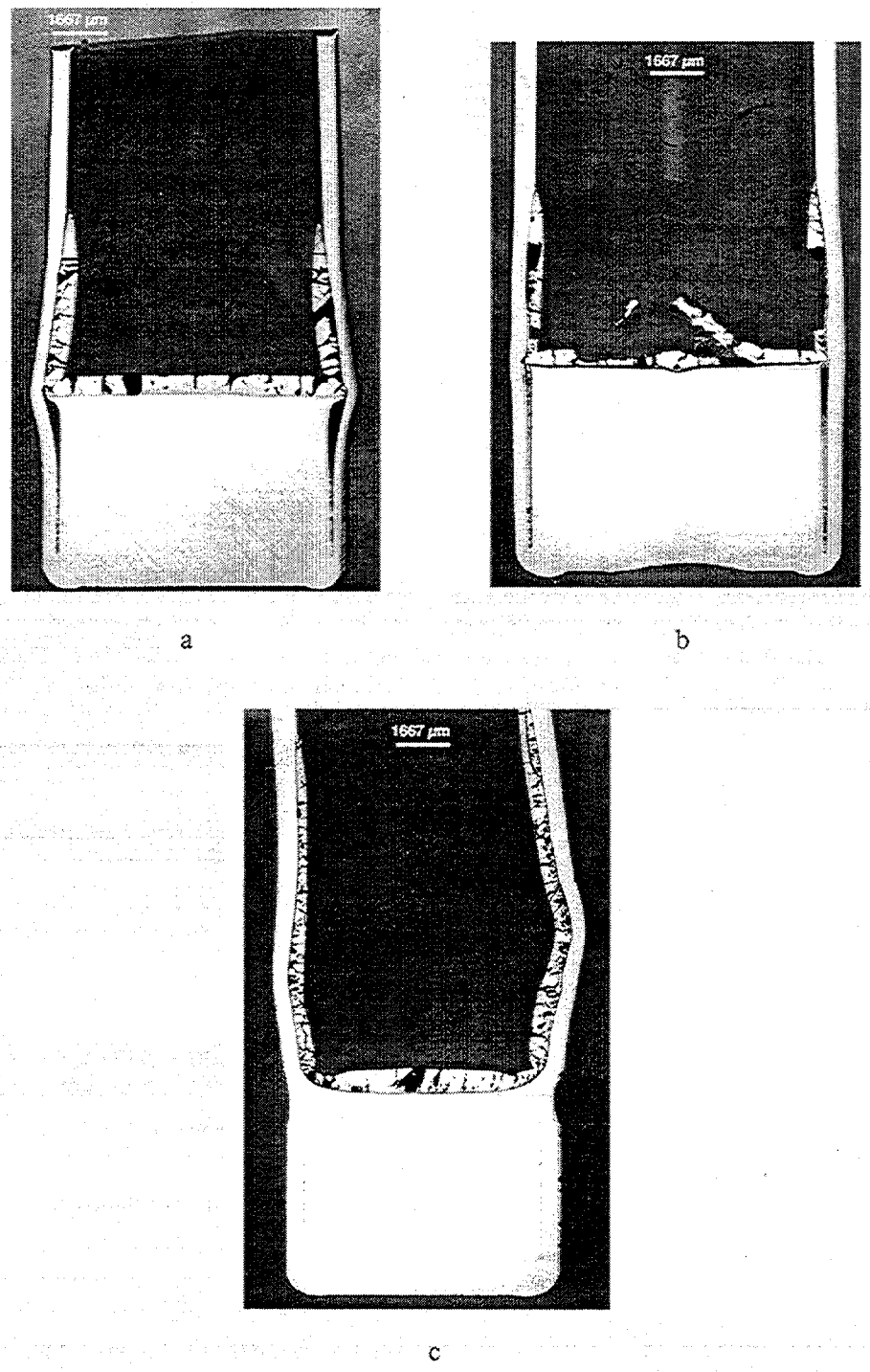

Fig. 7. Cross sections of Zircaloy tubes after corrosion testing with excess gallium (Ga) at 500°C for 200 h showing dimensional distortion. Distortion from formation of Zr_xGa_y is independent of welding technique. a = LBW, 0.5 g Ga; b = EBW, 0.5 g Ga; c = no crevice, 0.6 g Ga.

even though there was considerable empty space remaining within the capsule at the end of the test (Fig. 8). One of the Zircaloy materials showed little or no distortion even at the highest amounts of gallium, despite the fact that a Zr_xGa_y type of IC formed. Comparisons of the corrosion products at high magnifications showed some differences in the appearance of the ICs. Where no distortion occurred, the corrosion product was more porous than where distortion did occur (Fig. 9).

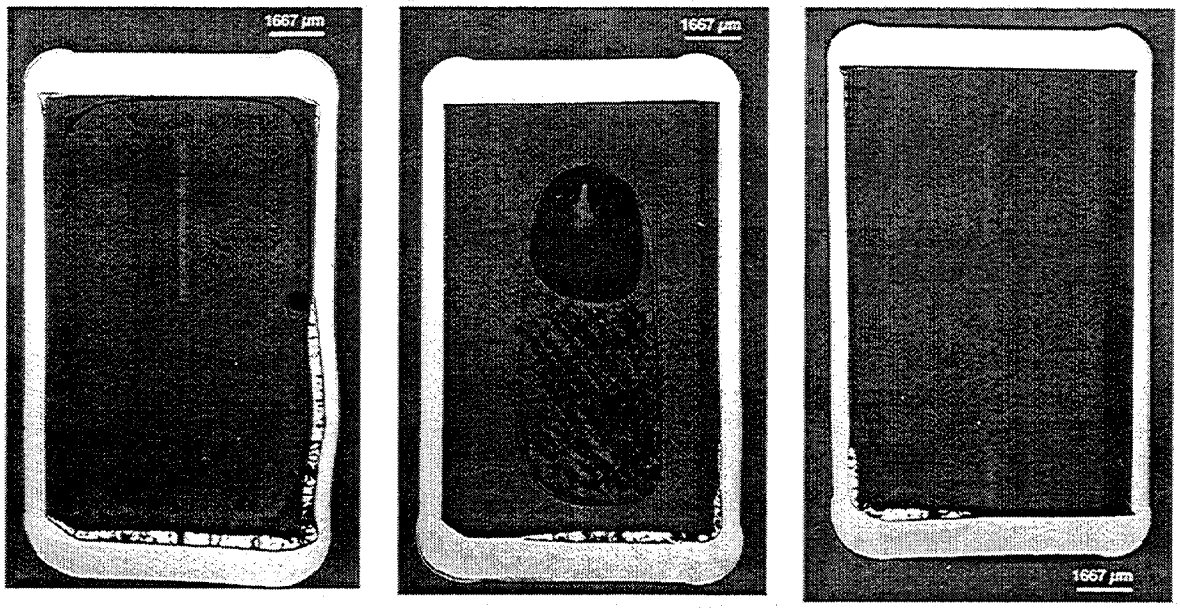

a b c

Fig. 8. Corrosion testing with smaller amounts of gallium (Ga) at 500°C for 200 h. a = 0.2 g Ga, shows a small amount of dimensional distortion; b = 0.09 g Ga, shows minor dimensional distortion; c = 0.05 g Ga, shows no dimensional distortion.

The results of hardness measurements across the reaction zones are shown in Table 2. The reaction zones have hardness numbers significantly higher than those for the base metal. In all cases, as would be expected, the hardness numbers for the porous layers were less than those for the layers between the porous layer and the base metal. Because of the large standard deviations associated with these numbers, no inferences can be made with respect to susceptibility to distortion.

Further testing at temperatures below 500°C showed that, in the susceptible materials, dimensional distortion also occurred at 400 and 350°C but was not found after 200 h at 300°C. After 200 h at 300°C, there was a large amount of unreacted gallium in the capsule at the end of the test. The rate of reaction is very slow at ≤300°C, evidenced by the decreasing amount of corrosion product formed at ≤200 h (Fig. 10).

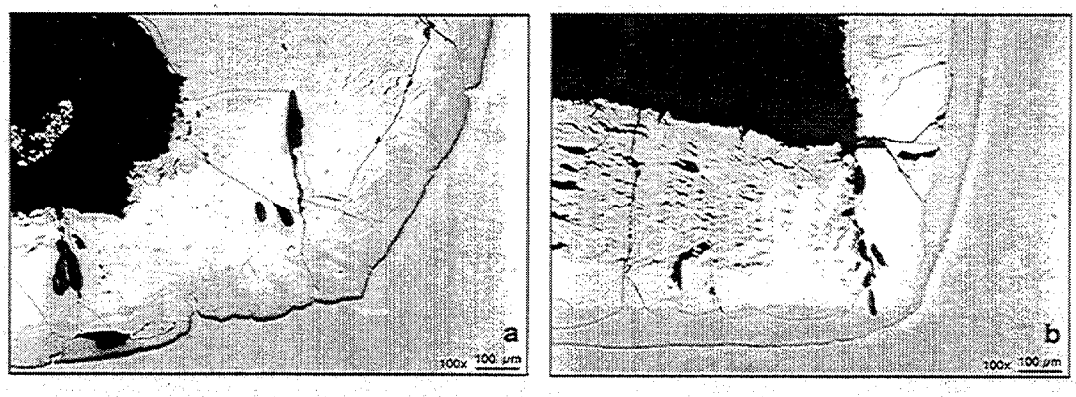

Fig. 9. Porosity in Zr_xGa_y formed at 500°C in Zircaloy material. a, material that distorted; b, material that did not distort.

Table 2. Vicker hardness (25 g load) for Zircaloys after 200 h at 500°C with gallium

Material	Porous layer	Layer adjacent to porous layer	Layer Difference	Base Metal
Zircaloy A	397 ± 49[a]	776 ± 58	379	190 ± 5
Zircaloy B	691 ± 236	1136 ± 25	445	167 ± 5
Zircaloy C	406 ± 62	887 ± 119	481	188 ± 7

[a] Standard deviation.

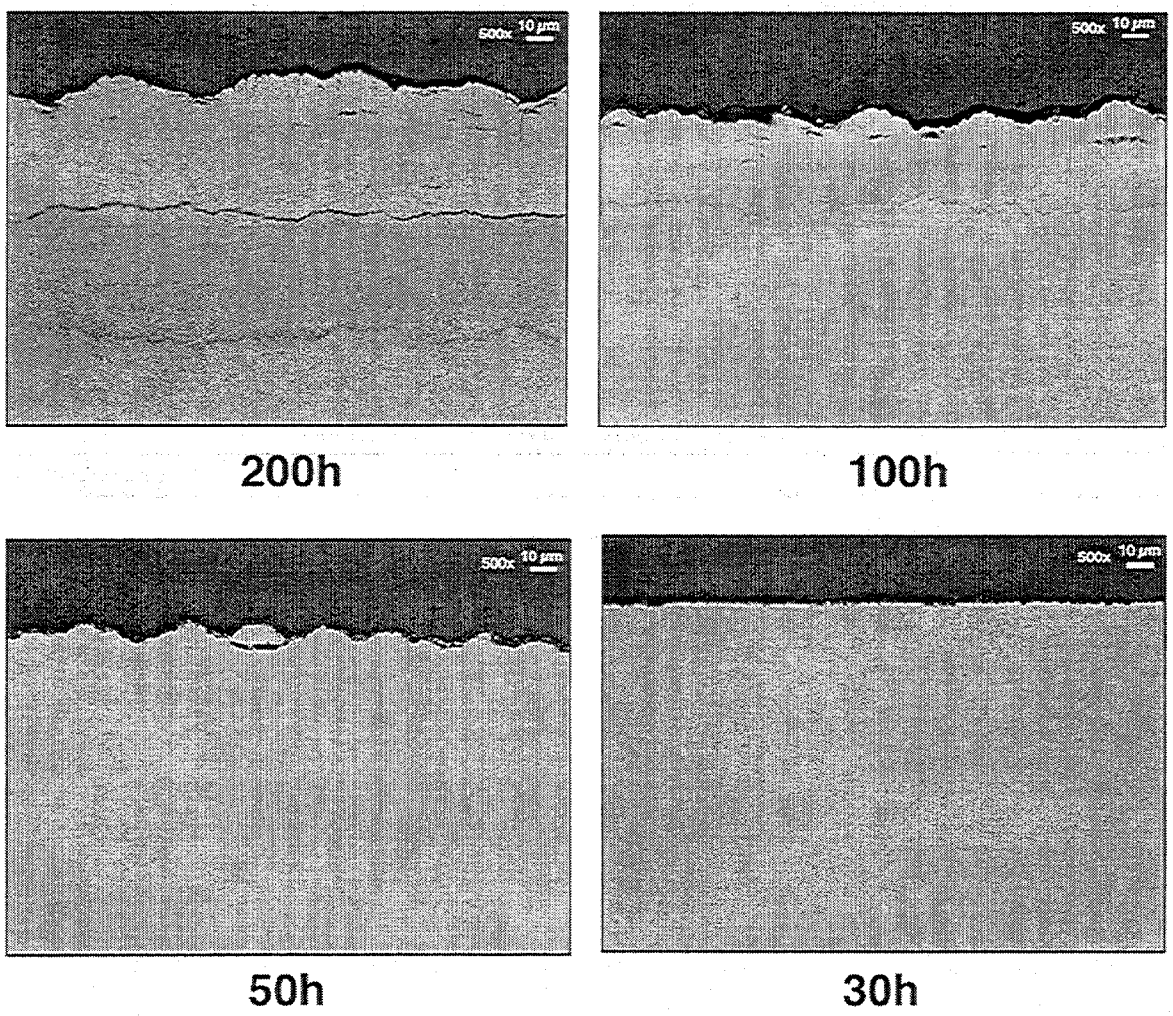

Fig. 10. At 300°C, ICF decreases with decreasing time of exposure.

As indicated in Fig. 8, dimensional distortion at 500°C was eliminated when smaller amounts of gallium were used in the capsule. In subsequent tests at 500°C with even smaller quantities of gallium (0.025 to 0.00038 g), ICF was localized to specific regions where gallium chemically wet the capsule wall but the depth of interaction was quite shallow (Fig. 11).

In subsequent tensile tests, it was noted that the Zircaloy material that resisted distortion was somewhat weaker than the other two materials, and its tensile properties were unchanged after exposure at 300 or 500°C. The two stronger materials became weaker and more ductile after heat treatment at 500°C, suggesting that this heat treatment might be used to reduce susceptibility to distortion. However, exposure to gallium at 500°C continued to produce distortion in these materials even after a preexposure heat treatment for 200 h at 500°C.

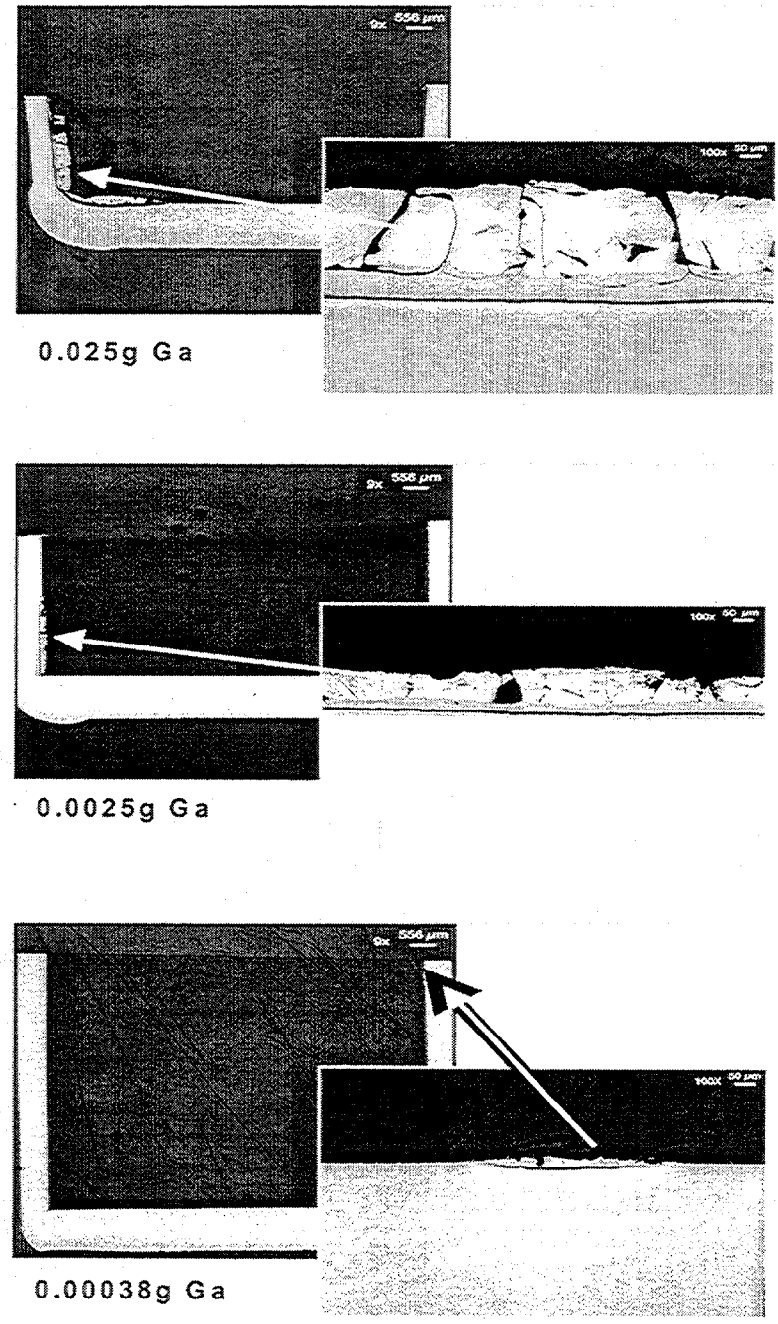

Fig. 11. ICF continues to decrease as the mass of gallium is decreased.

4.1.2 LME Tests

CERT tests (3.33×10^{-6}/s) were conducted in gallium at 30 and 100°C, and the results (average of three specimens per condition) are shown in Figs. 12 to 17. No differences in the tensile properties were found between the tests in gallium compared with those at the same

temperature without gallium. Although there was a small decrease in strength from 30 to 100°C, this same change occurred without gallium as well. Furthermore, the specimens all failed in a ductile manner, as shown in Fig. 18.

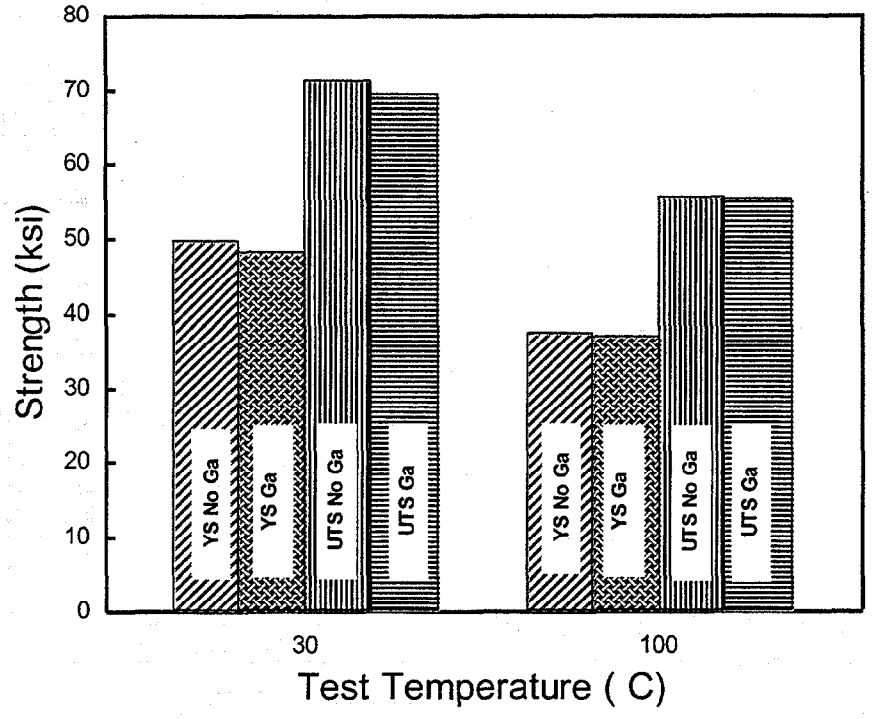

Fig. 12. LME tests showed no significant difference in strength for Zircaloy A at 30 and 100°C. YS, yield strength; UTS, ultimate tensile strength.

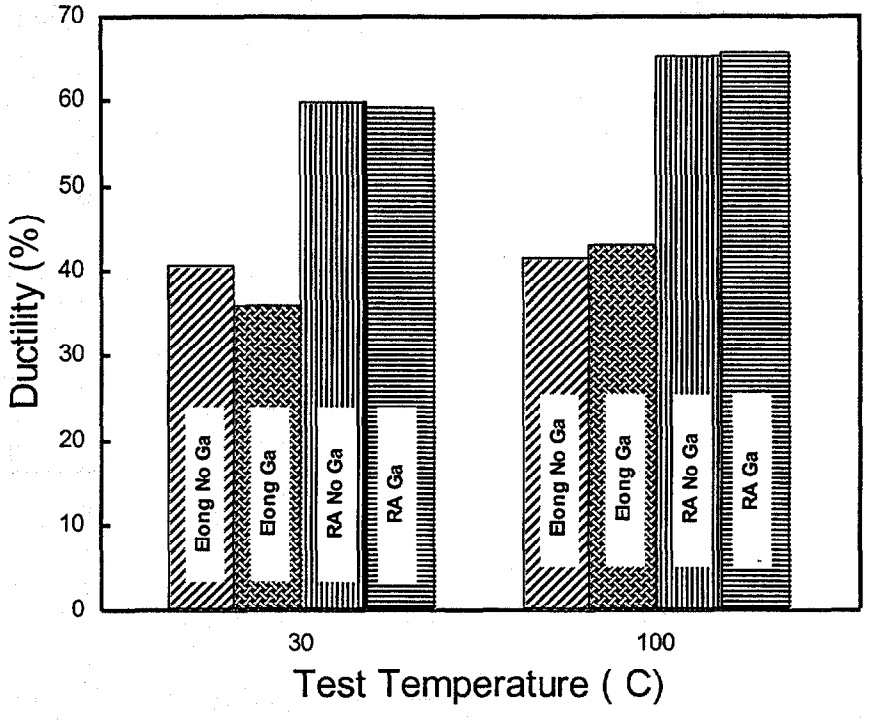

Fig. 13 . LME tests showed no significant difference in ductility for Zircaloy A at 30 and 100°C. Elong, elongation; RA, reduction in cross sectional area.

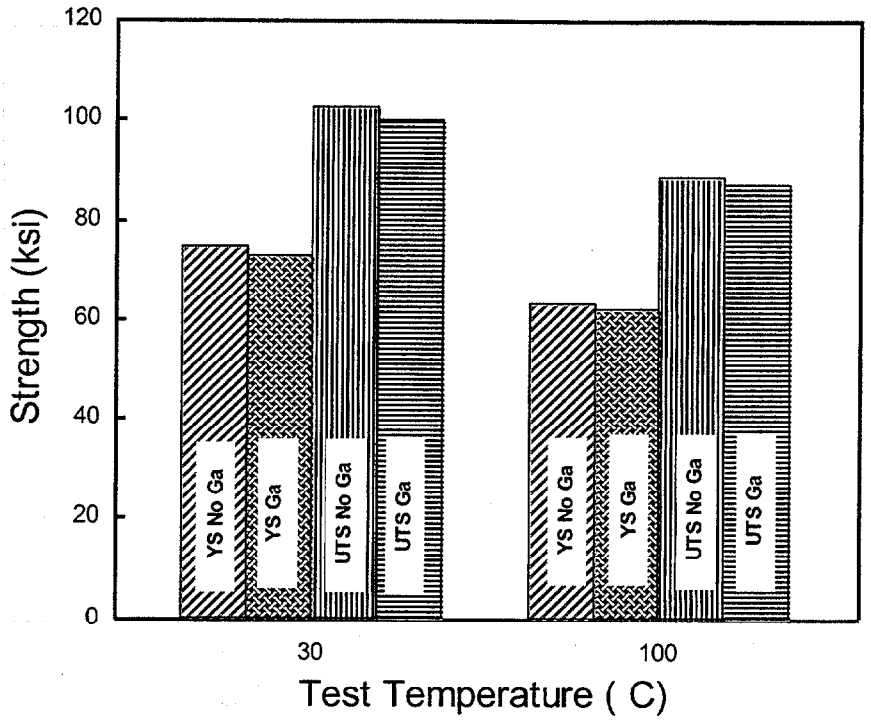

Fig. 14. LME tests showed no significant difference in strength for Zircaloy B at 30 and 100°C. YS, yield strength; UTS, ultimate tensile strength.

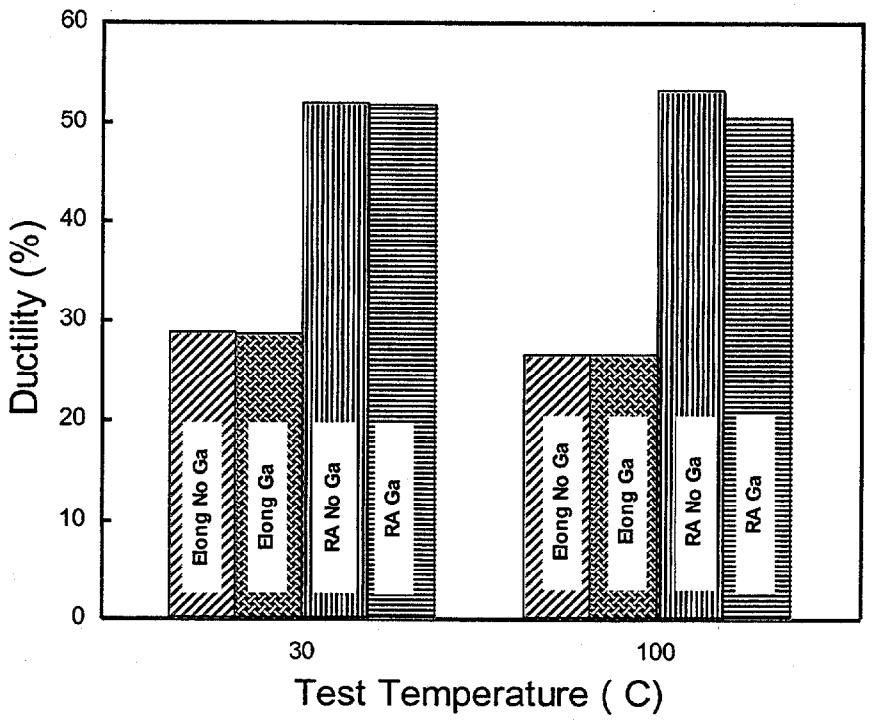

Fig. 15. LME tests showed no significant difference in ductility for Zircaloy B at 30 and 100°C. Elong, elongation; RA, reduction in cross sectional area.

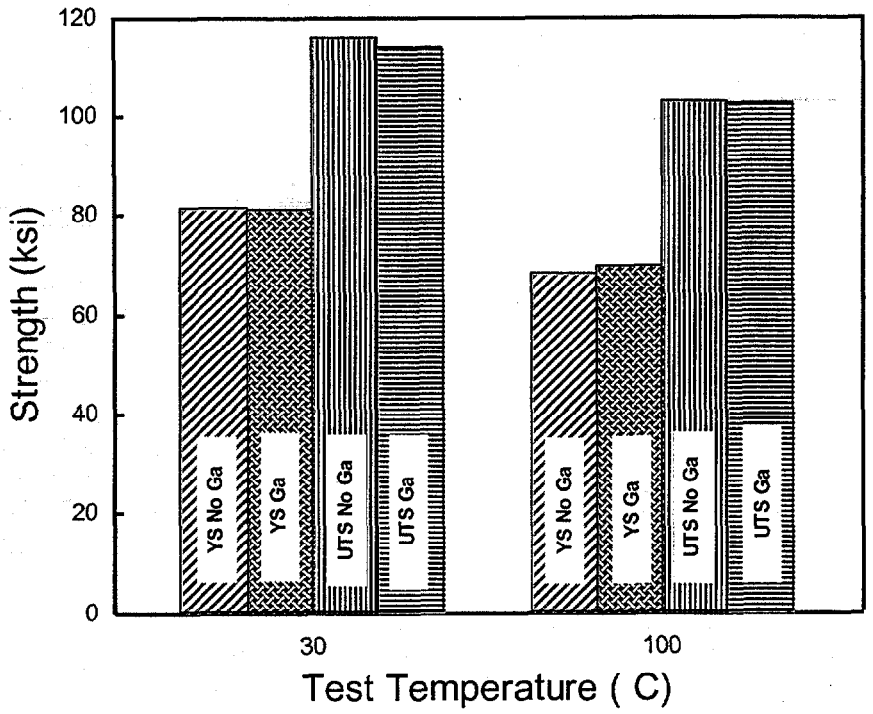

Fig. 16. LME test showed no change in strength for Zircaloy C at 30 and 100°C. YS, yield strength; UTS, ultimate tensile strength.

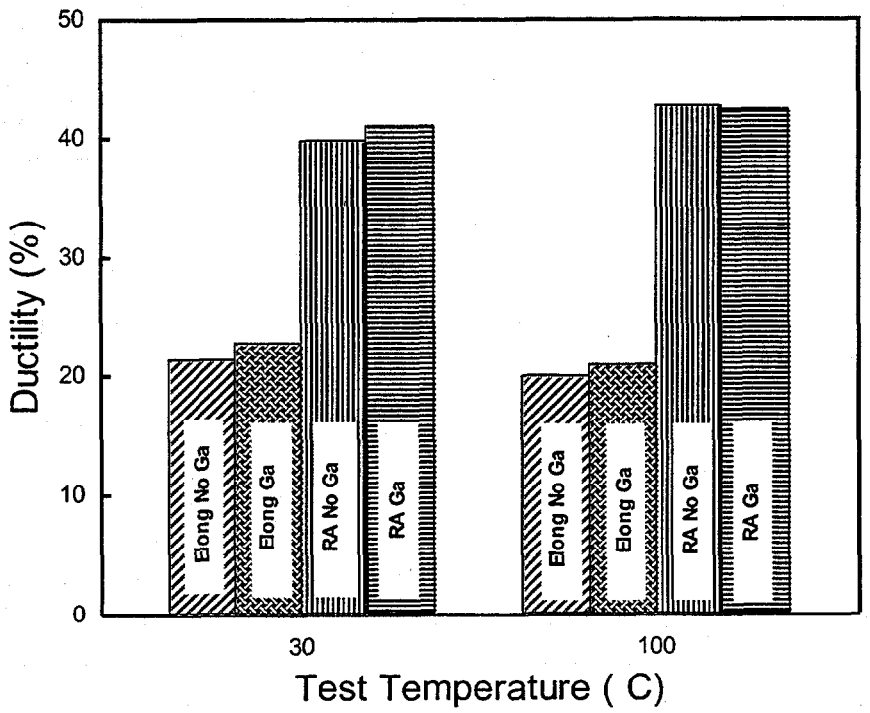

Fig. 17. LME tests showed no significant difference in ductility for Zircaloy C at 30 and 100°C. Elong, elongation; RA, reduction in cross sectional area.

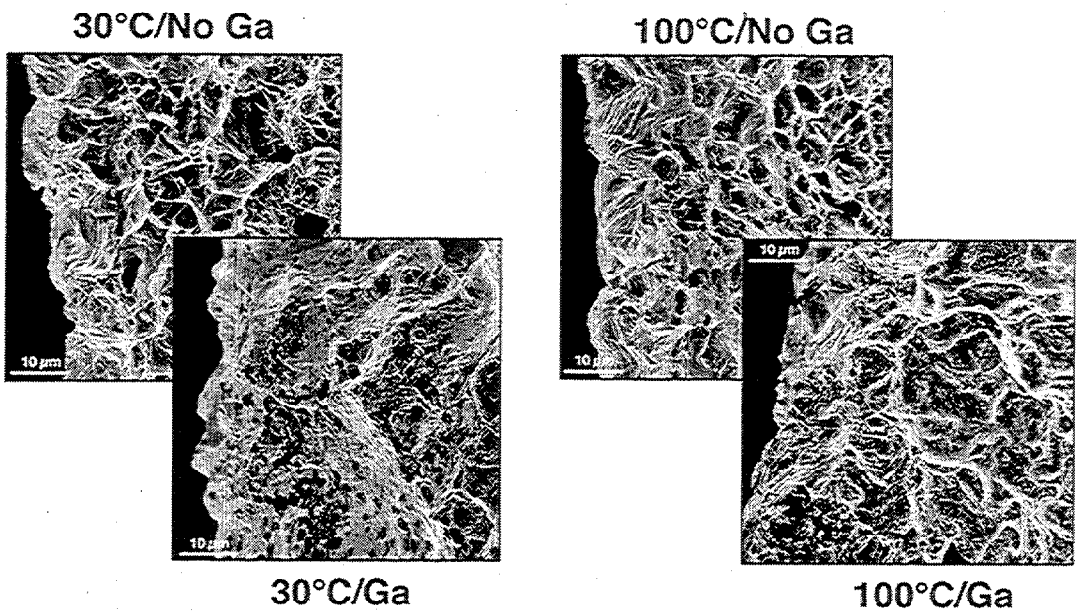

Fig. 18. Ductile failure mode at 30 and 100°C with and without gallium.

4.1.3 Corrosion-Mechanical Tests

The purpose of these tests was to obtain some measure of the effect of ICF on the mechanical properties of Zircaloy. The Zr_xGa_y IC is quite hard and brittle; therefore, significant (and unrealistically large) quantities of ICF would be expected to markedly affect the mechanical properties of the Zircaloy. Furthermore, as reported previously, distortion of Zircaloy at 500°C became a complicating factor. Based on prior data from the corrosion tests, exposure of the Zircaloy to gallium for 30 h at 300°C was ultimately selected as the condition for the corrosion portion of the corrosion-mechanical tests. Under these conditions, most of the gallium did not react with the Zircaloy; however, a thin, intermittent area of ICF was present along the gage length of the Zircaloy capsule specimen. CERT tests (8.33×10^{-4}/s) were conducted at room temperature and at 300°C. The results (average of three specimens per material, per condition) are shown in Figs. 19 and 20 and indicate very little, if any, effect of the formation of small amounts of ICF on the mechanical properties of Zircaloy. In addition, examination of the fracture surfaces did not indicate any significant difference in the mode of failure (Fig. 21).

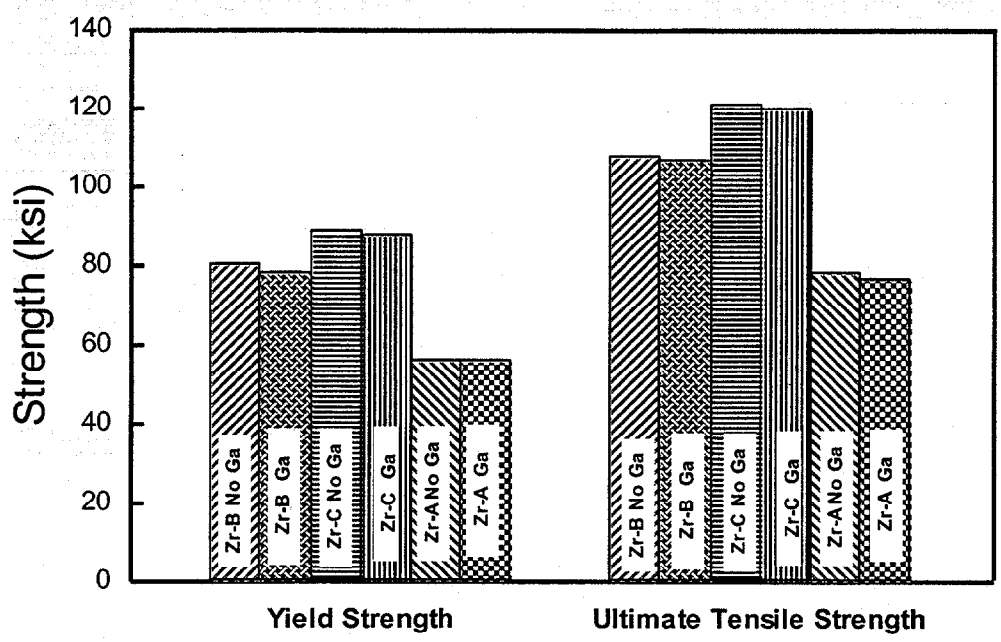

Fig. 19. No change in strength observed after reaction with gallium for 30 h at 300°C.

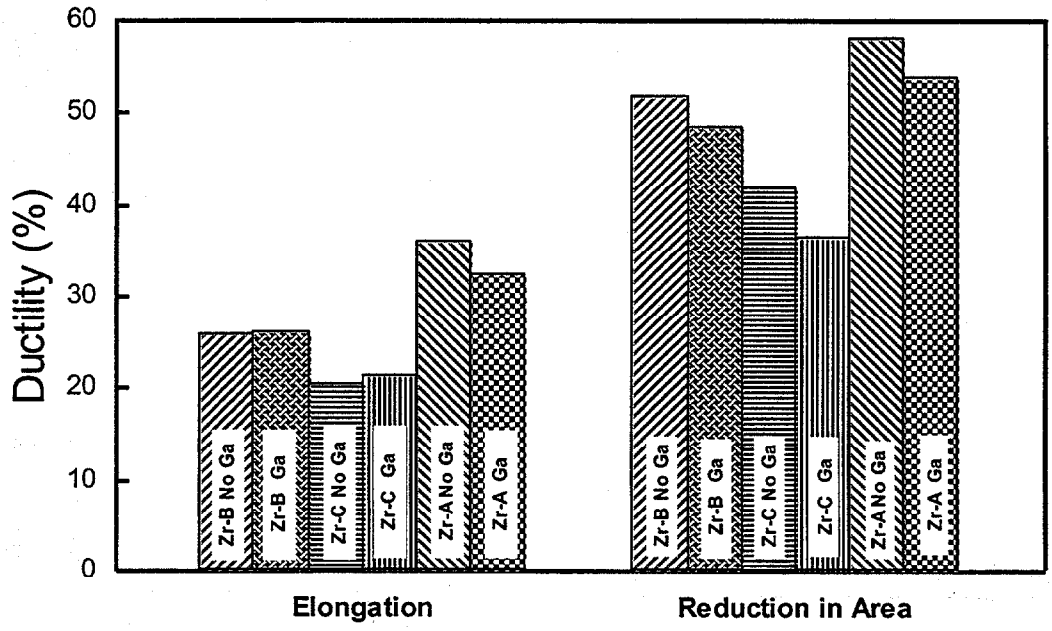

Fig. 20. No significant change in ductility observed after exposure to gallium for 30 h at 300°C.

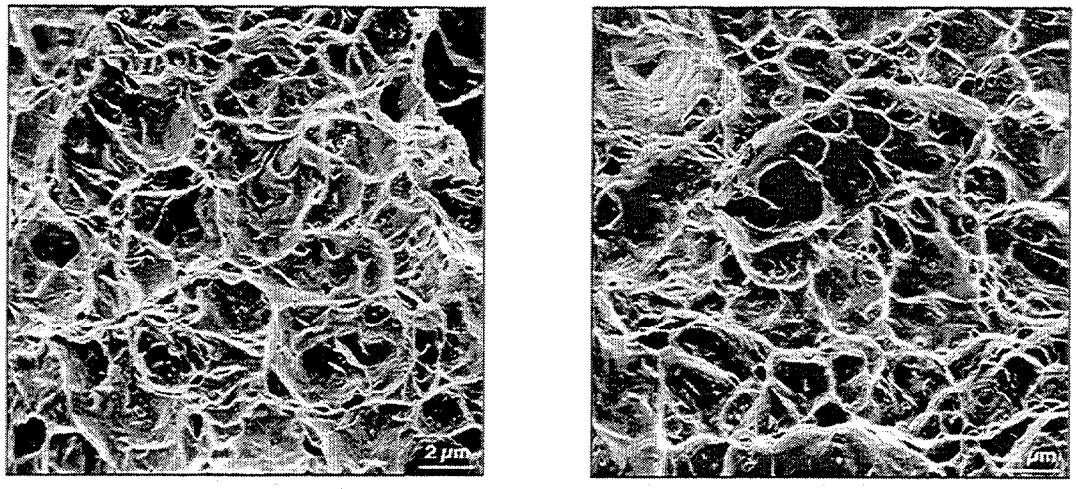

Fig. 21. Ductile fracture observed after 30 h at 300°C without and with gallium. Specimen mechanically tested at room temperature.

4.2 PHASE II

4.2.1 Corrosion Tests

Corrosion tests in nonprototypic, powder mixtures containing Ga_2O_3 were conducted at 300, 500, and 700°C for 6 and 12 weeks. Ce_2O_3 powder was mechanically blended with Ga_2O_3 powder to produce mixtures that contained 100, 1, 0.2, 0.1, and 0 wt % Ga_2O_3 to assess the effect of the concentration of gallium present during the exposures. Before initiating these tests, several surrogate oxides (for PuO_2) were tested at 500 or 700°C with Zircaloy: ZrO_2, CaO, and Ce_2O_3, as well as Ga_2O_3. In all cases, as would also occur with PuO_2,[1] an oxide layer was found on the inner surface of the Zircaloy that was qualitatively identified as ZrO_2 (Fig. 22).

In the matrix tests, there were significant differences among results at the three temperatures. At 300°C, no significant reaction was noted except for very slight surface roughening, even after the 12-week exposures (Fig. 23). At 500°C, the oxide layer mentioned previously was observed in all of the tests (Fig. 24). The thickness of the oxide layer was independent of Ga_2O_3 concentration and did not appreciably increase with time between 6 and 12 weeks. A visually distinguishable zone can be noted below the oxide layer. Although this zone was larger for the tests with 100% Ga_2O_3, there was no appreciable difference among 1, 0.2, and 0.1% Ga_2O_3 exposures.

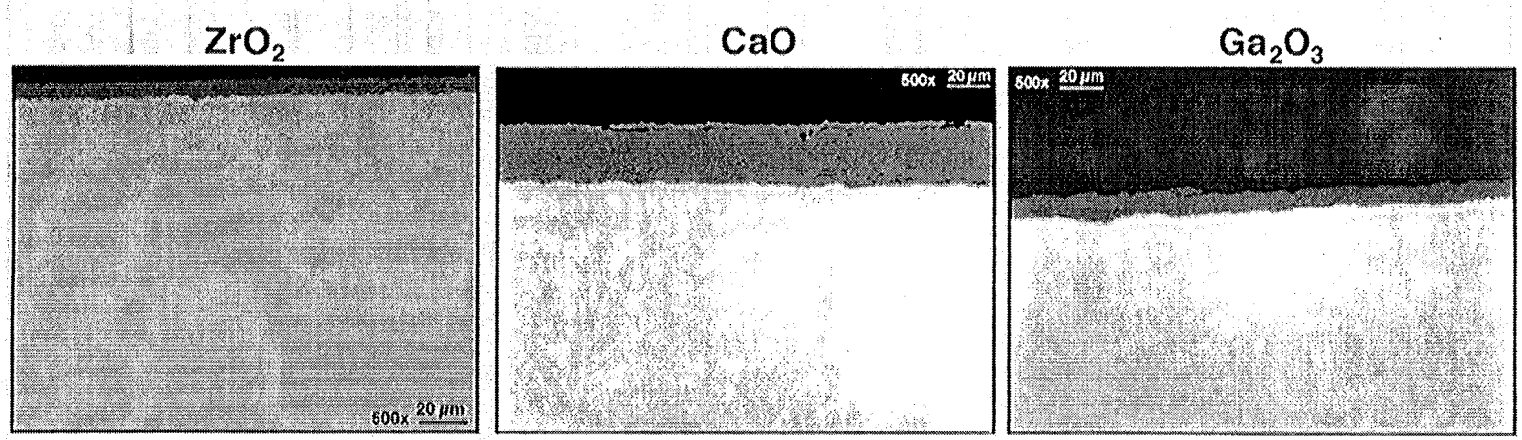

Fig. 22. Zircaloy reacts with oxides at 500°C to form zirconium oxide. Zirconium oxide formation is not limited to reaction of Zircaloy with Ga_2O_3.

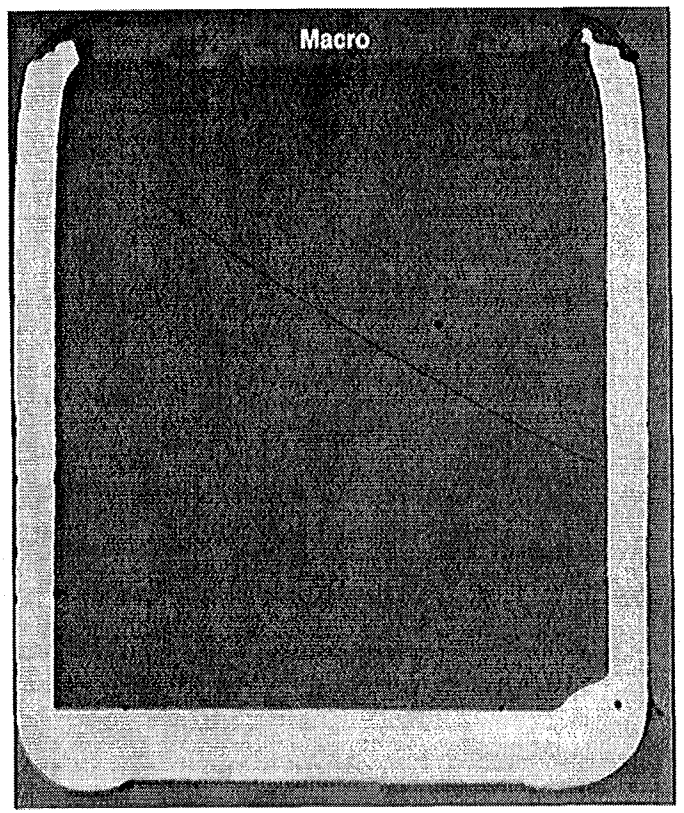

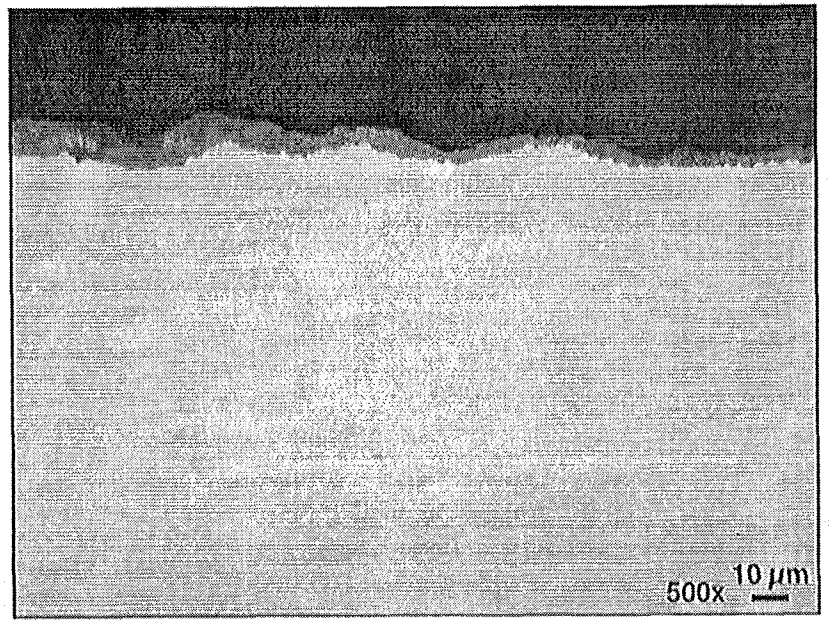

Fig. 23. No significant reaction of Zircaloy with Ga_2O_3 after 12 weeks at 300°C.

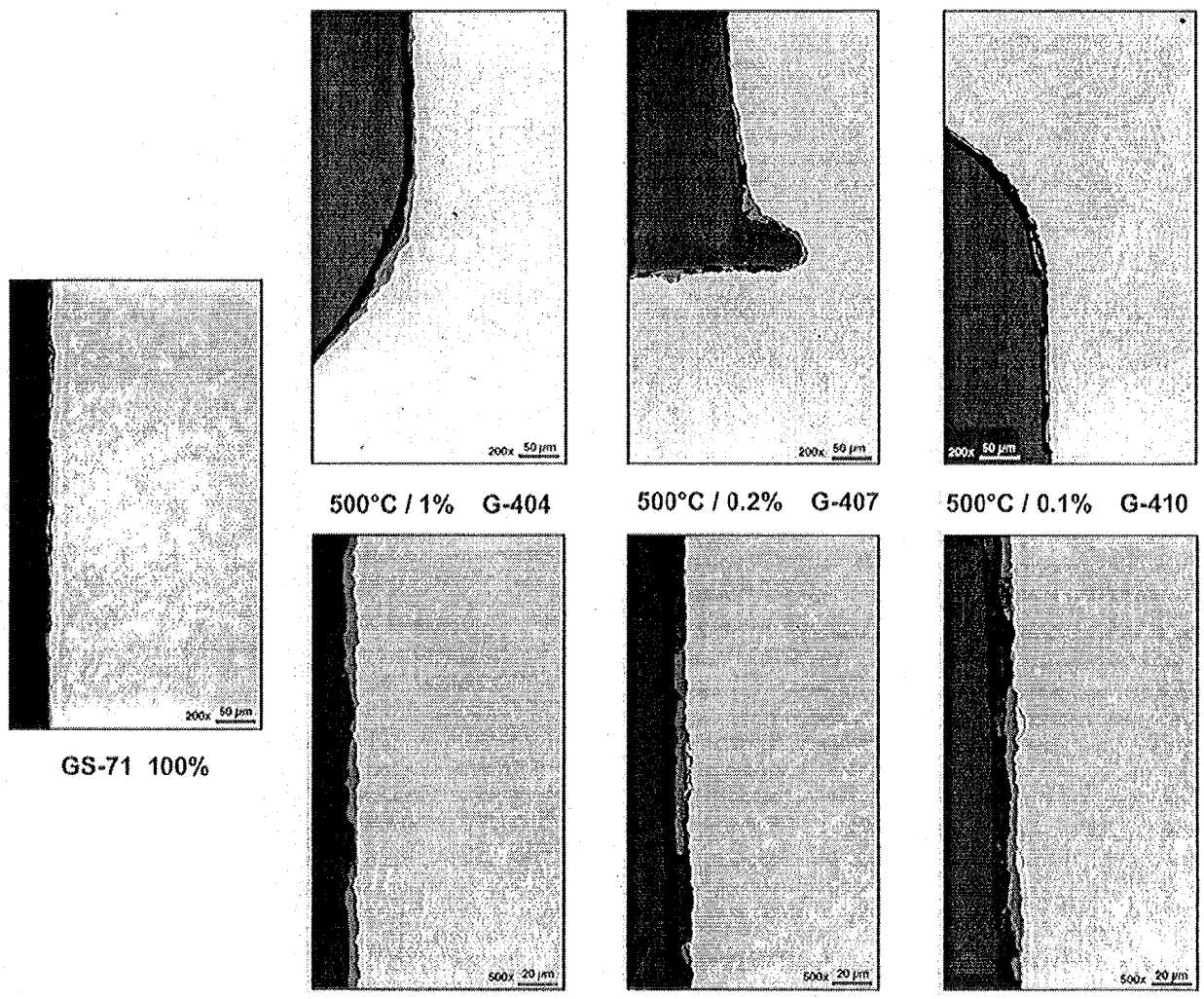

Fig. 24. Oxide layer present at 500°C for all ratios of Ga_2O_3 to cerium oxide.

At 700°C, there was formation of an oxide layer on the inner surface of the Zircaloy and an identifiable gallium-rich zone below the oxide layer. The thickness of both the oxide and gallium-rich zone increased with time, but the gallium-rich zone was visible only with 100% Ga_2O_3 (Fig. 25). Another feature not seen at 500°C is cracking of the Zircaloy. Generally, testing at 700°C resulted in a somewhat uniform distortion of the Zircaloy tubing, and the cracks may be associated with an oxygen-enriched zone.

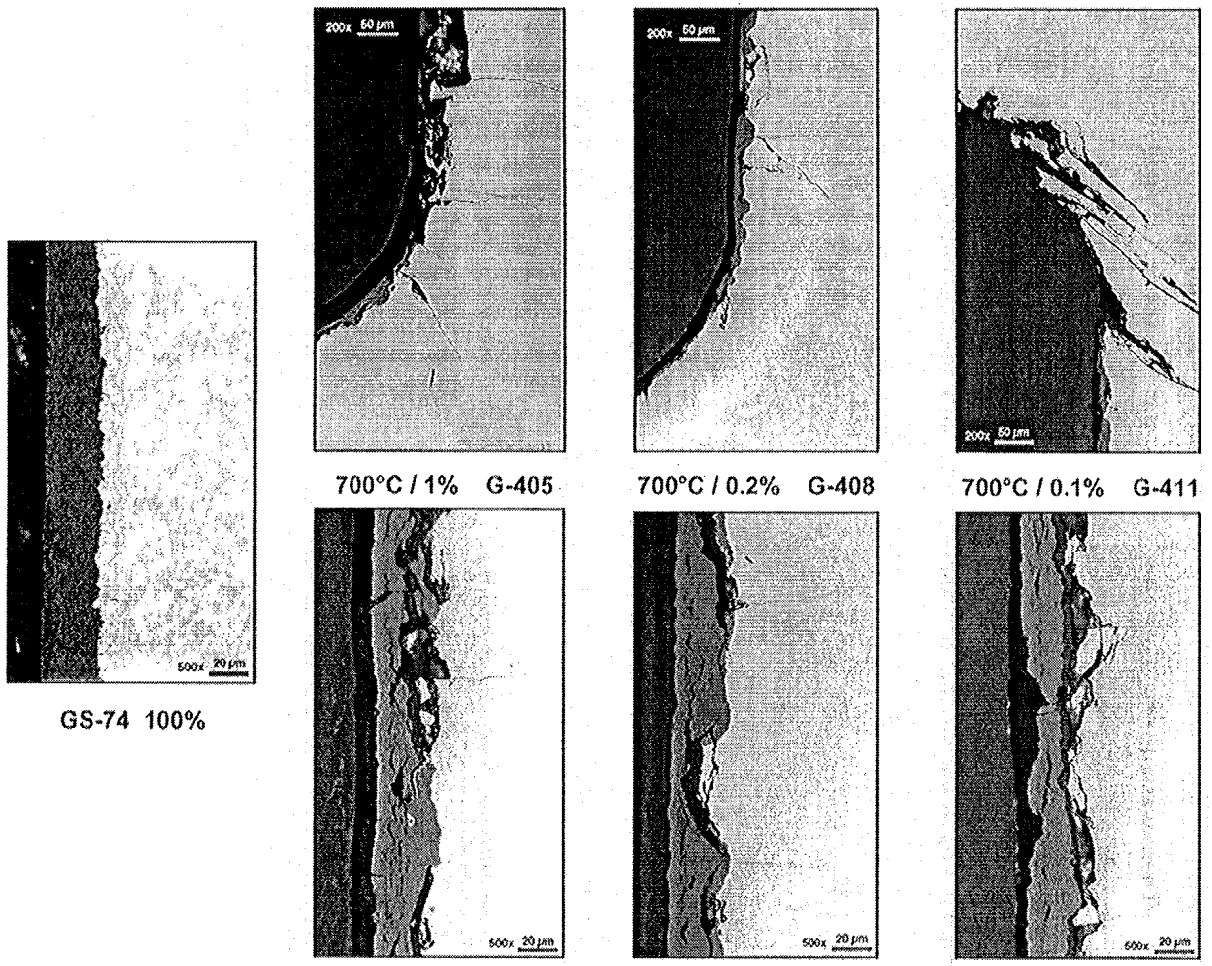

Fig. 25. Zr_xGa_y identified below the zirconium oxide layer after exposure to 100% Ga_2O_3 at 700°C.

4.2.2 Corrosion-Mechanical Tests

This portion of the testing program was aimed at determining the effect of exposures at 300 and 500°C of Zircaloy to oxide powders containing Ga_2O_3. Mechanical tests were not conducted after exposure at 700°C due to distortion (caused by creep) of the test specimens.

4.2.2.1 Room-Temperature Mechanical Tests

The results of CERT tests (8.33×10^{-4}/s), conducted at room temperature, are shown in Figs. 26 to 31. There was either a slight change or no change in the room-temperature tensile properties (three specimens per condition) of any of the Zircaloy materials after exposure at 300°C, as would have been predicted based on the corrosion test results reported previously. Similarly, after exposure at 500°C, there was little change in the room-temperature properties as a function of Ga_2O_2 concentration, but both room temperature yield and ultimate tensile strength (Figs. 28 and 30) were lower than at 300°C for two of the three Zircaloys for all Ga_2O_3 concentrations, with a corresponding increase in ductility as measured by elongation and reduction in area (Figs. 29 and 31). After exposure at 500°C, one of the Zircaloys had properties similar to those exhibited at 300°C except that ductility trended lower with exposure to powders with higher Ga_2O_3 (Figs. 26 and 27). Control tests indicated that these changes are a result of heat treatment at 500°C instead of the test environment. Before heat treatment at 500°C, the alloys (Zircaloys B and C) shown in Figs. 28 to 31 had room-temperature tensile properties similar to those shown for heat treating/exposure to oxide powder at 300°C. Thus, the heat treatment of these alloys at 500°C reduced their strength and increased their ductility. The properties of Zircaloy A (Fig. 26) were little changed by the 500°C heat treatment.

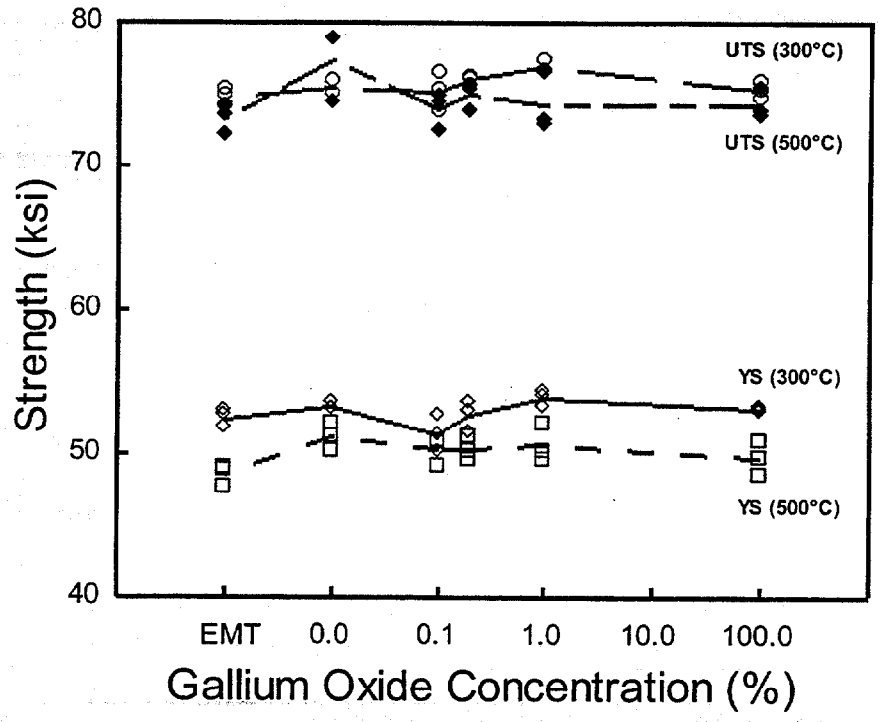

Fig. 26. No significant change in room-temperature strength for Zircaloy A after exposure to Ga_2O_3 in cerium oxide (6 weeks at 300 and 500°C). YS, yield strength; UTS, ultimate tensile strength; EMT, empty.

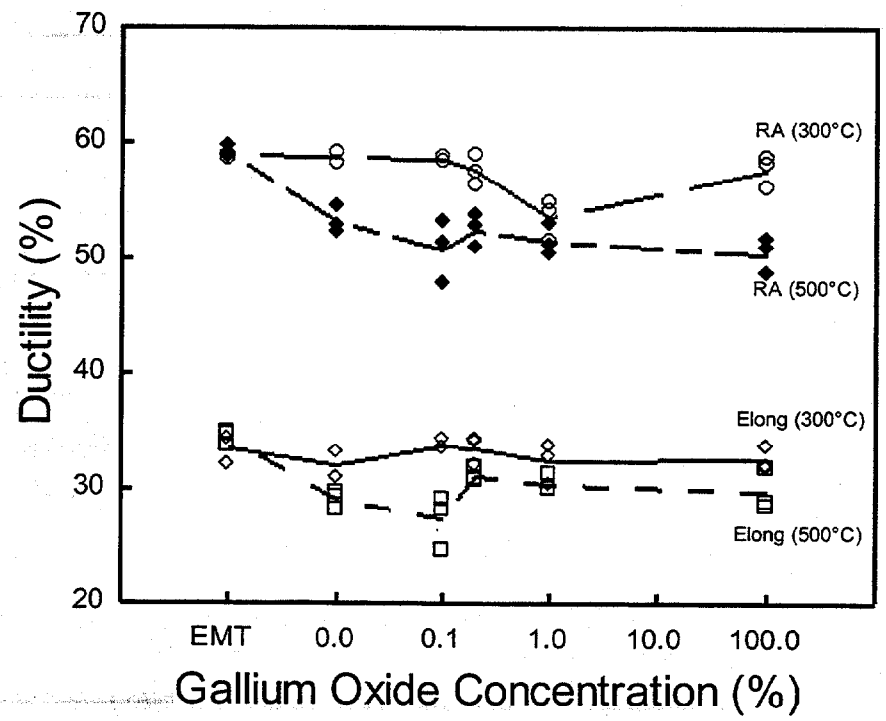

Fig. 27. Slight change in room-temperature ductility for Zircaloy A after exposure to Ga_2O_3 in cerium oxide (6 weeks at 300 and 500°C). Elong, elongation; RA, reduction in cross-sectional area; EMT, empty.

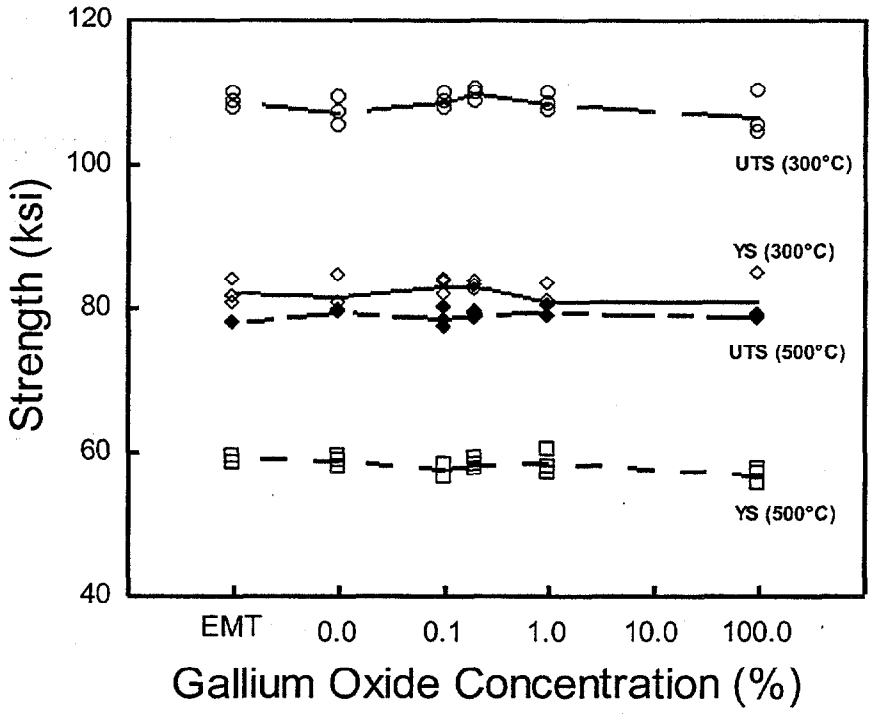

Fig. 28. No significant change in room-temperature strength for Zircaloy B after exposure to Ga_2O_3 in cerium oxide (6 weeks at 300 and 500°C). YS, yield strength; UTS, ultimate tensile strength; EMT, empty.

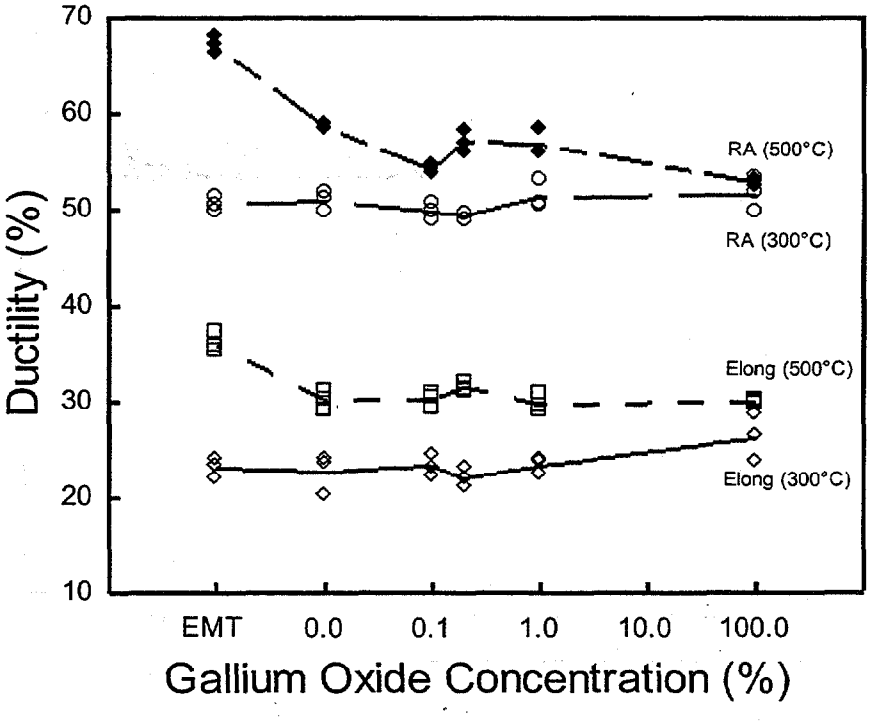

Fig. 29. Slight change in room-temperature ductility for Zircaloy B after exposure to Ga_2O_3 in cerium oxide (6 weeks at 300 and 500°C). Elong, elongation; RA, reduction in cross-sectional area; EMT, empty.

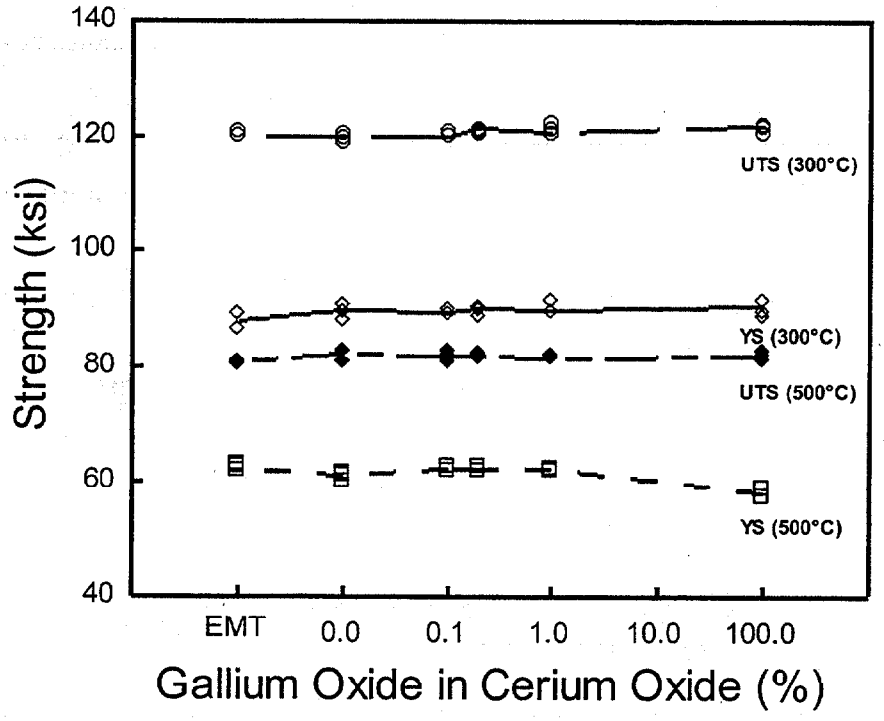

Fig. 30. No significant change in room-temperature strength for Zircaloy C after exposure to Ga_2O_3 in cerium oxide (6 weeks at 300 and 500°C). YS, yield strength; UTS, ultimate tensile strength; EMT, empty.

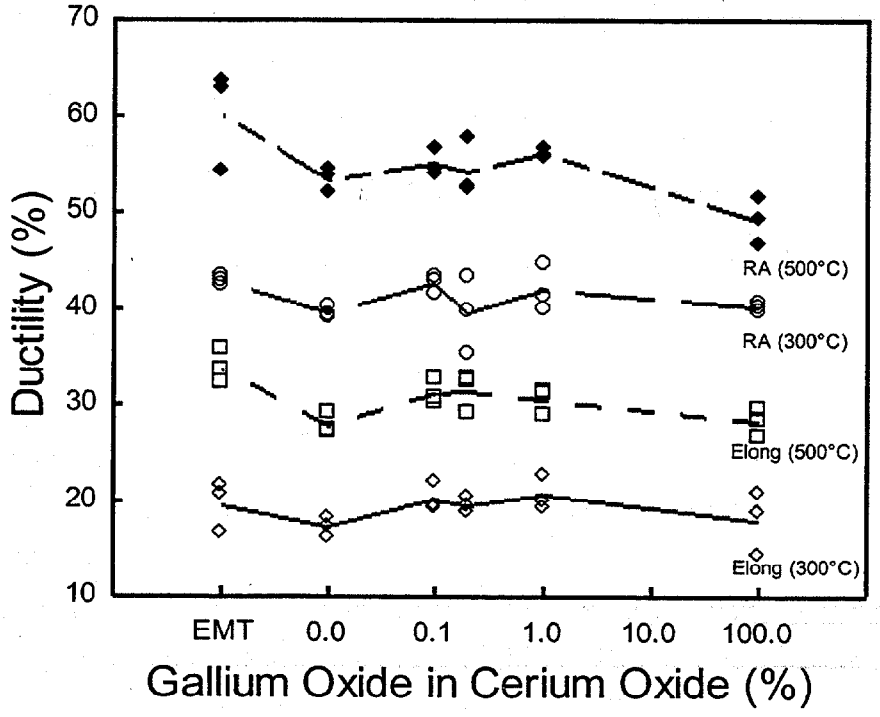

Fig. 31 . Slight change in room-temperature ductility for Zircaloy C after exposure to Ga_2O_3 in cerium oxide (6 weeks at 300 and 500°C). Elong, elongation; RA, reduction in cross-sectional area; EMT, empty.

4.2.2.2 High-Temperature Mechanical Tests

CERT tests (8.33×10^{-4}/s) were conducted at 300 and 500°C. As shown in Fig. 32, there is little, if any, change in the 300°C strength and ductility properties (two specimens per condition) of Zircaloy A as a result of exposure to various concentration of Ga_2O_3. The mechanical properties of specimens after exposure are very similar to those for the heat-treated (without oxide) specimens. Compared with the room-temperature properties, the 300°C strength values are, as expected, lower and the ductility values are, as expected, slightly higher.

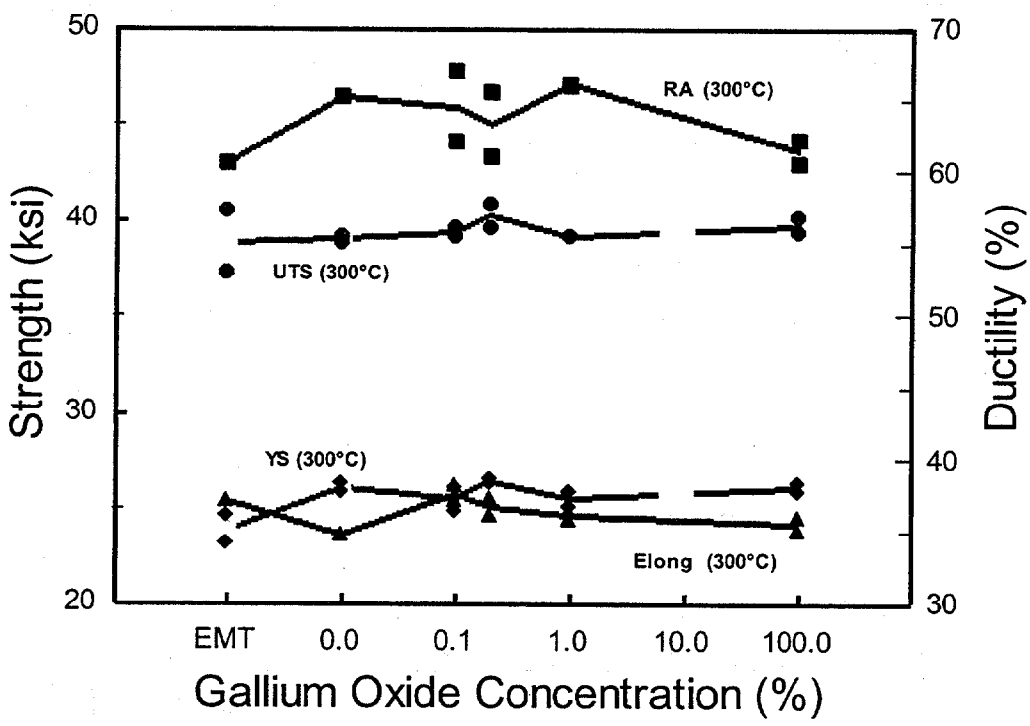

Fig. 32. No significant changes in 300°C strength and ductility for Zircaloy A after exposure to Ga_2O_3 in cerium oxide (6 weeks at 300°C). YS, yield strength; UTS, ultimate tensile strength; Elong, elongation; RA, reduction in cross-sectional area; EMT, empty.

As shown in Fig. 33, there is little, if any, change in the 500°C strength and ductility properties of Zircaloy A as a result of exposure to various concentrations of Ga_2O_3. The mechanical properties of specimens after exposure are very similar to those for the 500°C heat-treated (without oxide) specimens. Compared with the 300°C properties, the 500°C strength values are, as expected, lower and the ductility values are, as expected, slightly higher.

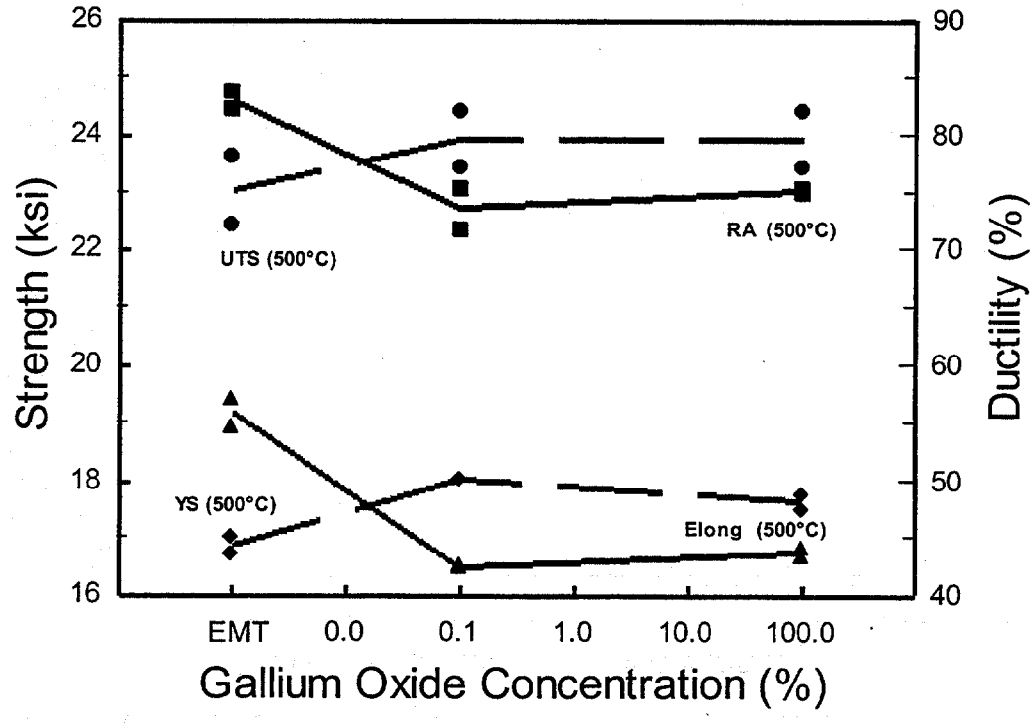

Fig. 33. No significant changes in 500°C strength and ductility for Zircaloy A after exposure to Ga_2O_3 in cerium oxide (6 weeks at 500°C). YS, yield strength; UTS, ultimate tensile strength; Elong, elongation; RA, reduction in cross-sectional area; EMT, empty.

Behavior similar to Zircaloy A was observed for the mechanical properties (two specimens per condition) of Zircaloy C at 300 and 500° (Figs. 34 and 35). While data were not obtained for Zircaloy B, it can be inferred that, within the limitations of 6-week tests, the high-temperature mechanical properties of Zircaloy materials are not affected by exposure to Ga_2O_3. The only effect that would be observed is due to time at temperature.

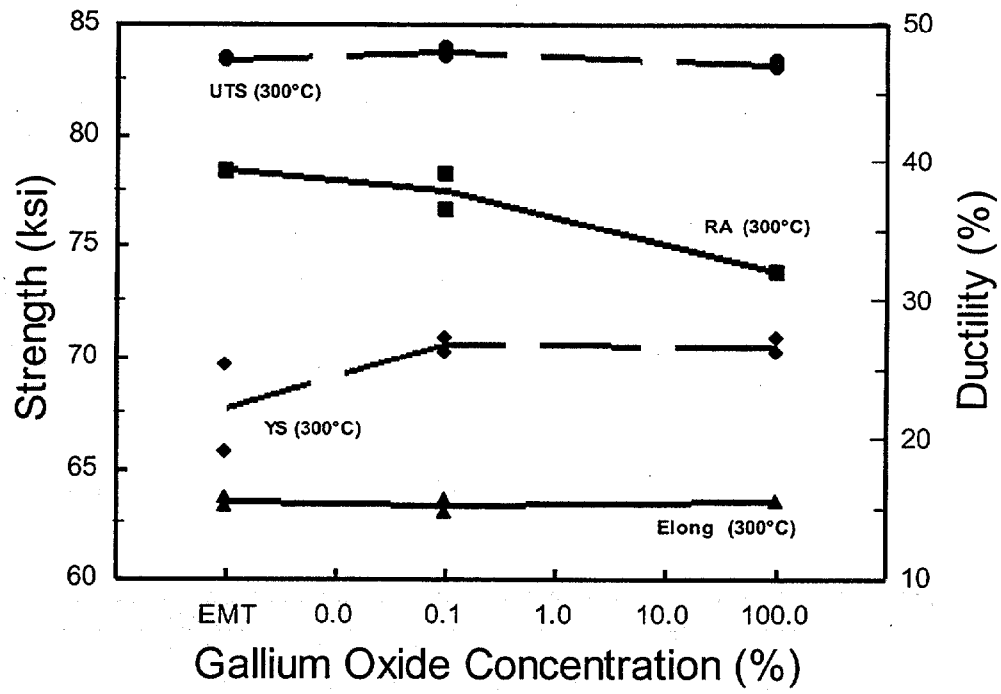

Fig. 34. No significant changes in 300°C strength and ductility for Zircaloy C after exposure to Ga_2O_3 in cerium oxide (6 weeks at 300°C). YS, yield strength; UTS, ultimate tensile strength; Elong, elongation; RA, reduction in cross-sectional area; EMT, empty.

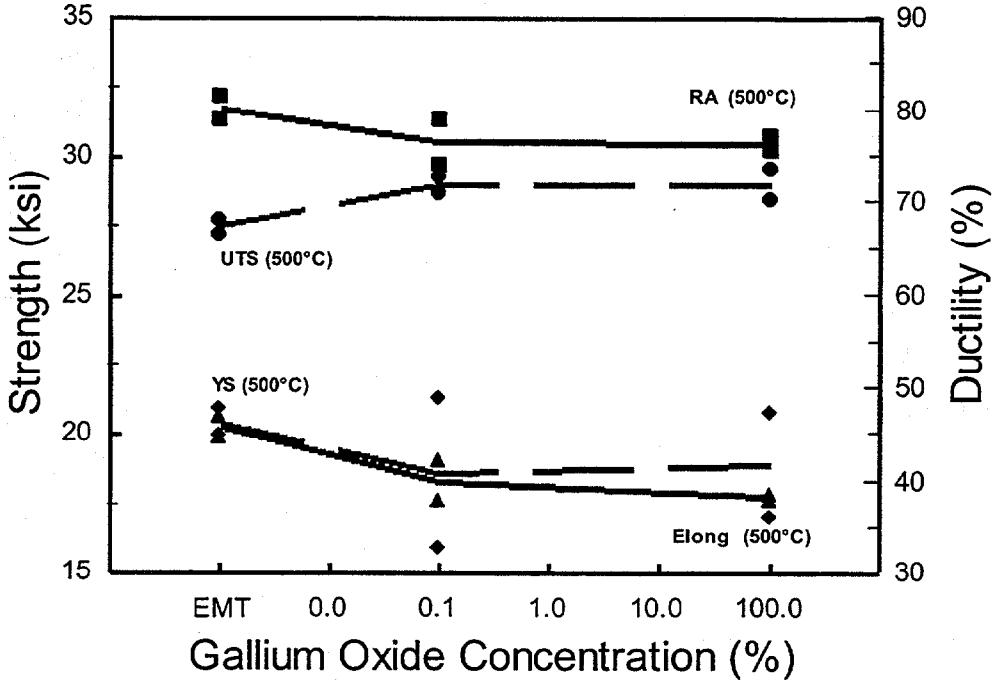

Fig. 35. No significant changes in 500°C strength and ductility for Zircaloy C after exposure to Ga_2O_3 in cerium oxide (6 weeks at 500°C). YS, yield strength; UTS, ultimate tensile strength; Elong, elongation; RA, reduction in cross-sectional area; EMT, empty.

5. DISCUSSION

Liquid gallium is highly reactive with most metals since it readily alloys with elemental components that are in many structural materials. For example, gallium forms intermetallic compounds with iron, nickel, chromium, cobalt, vanadium, and zirconium. Even though these elements have limited solubility in gallium at temperatures as high as ~500°C, they would not be suitable for use in structural materials to contain gallium above 300°C because of their chemical conversion to ICs of the form M_xGa_y, where M_x refers to a metallic element. However, in the present application, in which the total amount of gallium in a 3.66-m (12-ft) fuel pin is expected to be ~0.02 g, formation of ICs would be very limited. If in the unlikely event that all of the gallium present in a fuel pin were to reach the cladding interface in one location, only a very small amount of the cladding wall would be converted to ICs and the effect on tensile properties will be slight to negligible. These studies have also shown no embrittlement of Zircaloy caused by either classic LME effects from liquid gallium or reactions that result in the formation of small amounts of ICF or an oxide layer on the Zircaloy.

LME is a phenomenon similar to stress corrosion cracking that can occur with certain liquid metal–solid metal combinations. However, the kinetics and mechanisms of LME are not clearly understood. One explanation is that chemisorption of the liquid reduces bond cohesion at the surface,[14, 15] or that chemisorption creates dislocations at the tip of a crack that subsequently interact with the dislocation structure in the plastic zone leading to further microcracking.[16, 17] Wetting by the liquid metal and the presence of a tensile stress are necessary for LME to occur, but if the component elements form stable, high-melting-point compounds, severe LME is unlikely.[18, 19] Because zirconium readily forms a series of ICs with gallium at temperatures to 800°C, its resistance to LME is not surprising.

On the other hand, ICF results in conversion of zirconium in Zircaloy to a brittle intermetallic phase, which could affect the mechanical properties of the cladding. However, after reaction at 300°C to form a thin layer of IC on the inner diameter surface of the Zircaloy (but more than expected in a fuel pin), there was no effect on the tensile properties. When a similar experiment was conducted at 350°C and the thickness of the IC increased, a modest loss in ductility was found. This finding further supports a conclusion that gallium effects are mass limited.

The distortion that results from ICF appears to be related to stresses that develop in the wall of some Zircaloy tubing during interalloying. In preliminary tests at 400 to 600°C with either pure zirconium or nonvendor supplied Zircaloy II, no distortion was noted with quantities of liquid gallium that later caused distortion in two of the three vendor-supplied materials.

Differences associated with the type of Zircaloy tested were the appearance of much more porosity in the outer IC that formed and less cracking of the inner IC where distortion was not observed. In the materials where distortion occurred, the IC was more dense and exhibited numerous cracks usually in a direction perpendicular to the wall. As the quantity of gallium available to react with the Zircaloy was reduced, distortion was eliminated. For small quantities of gallium at ≥350°C, the liquid gallium is quickly consumed to locally form IC, thus ending the reaction. However, when additional (excess) gallium is available, further reaction can occur as the zirconium and gallium continue to react. It is very likely that liquid gallium either diffuses through the first IC that forms or reaches the metal-IC interface via cracks in the IC. It is during this process that stresses likely develop and lead to distortion. It is well known from oxidation studies that certain volume ratios of corrosion product (oxide) to metal can lead to tensile stresses in the metal.[20]

Most probably, though not certainly, gallium will be present in MOX fuel as an oxide rather than in metallic form.[1] In corrosion tests involving oxides (Ga_2O_3, Ce_2O_3, CaO, or ZrO_2) in contact with Zircaloy, formation of zirconium oxide at the metal-oxide interface was found at 500°C. With Ga_2O_3, gallium was present below the oxide at 500°C. At 700°C, Zr_xGa_y was identified below the oxide. Because zirconium forms a very stable oxide (Fig. 36), oxide formation on the fuel cladding inner diameter surface is likely, although the rate of formation at temperatures below 500°C is unknown (e.g., at 300°C there was very slight indication of oxide formation after 12 weeks).

The room-temperature, 300, and 500°C tensile test results after exposure to oxide (Ga_2O_3 in Ce_2O_3) for 6 weeks at 300 or 500°C (temperatures that bracket the expected LWR clad normal operating temperature of ~400°C) do not appear to indicate any appreciable effect of concentration of Ga_2O_3 on strength or ductility. Two of the Zircaloy materials showed significant changes in room-temperature properties from heat treatment at 500°C. However, but there were no further effects attributable to exposure to the various concentrations of Ga_2O_3 for 6 weeks.

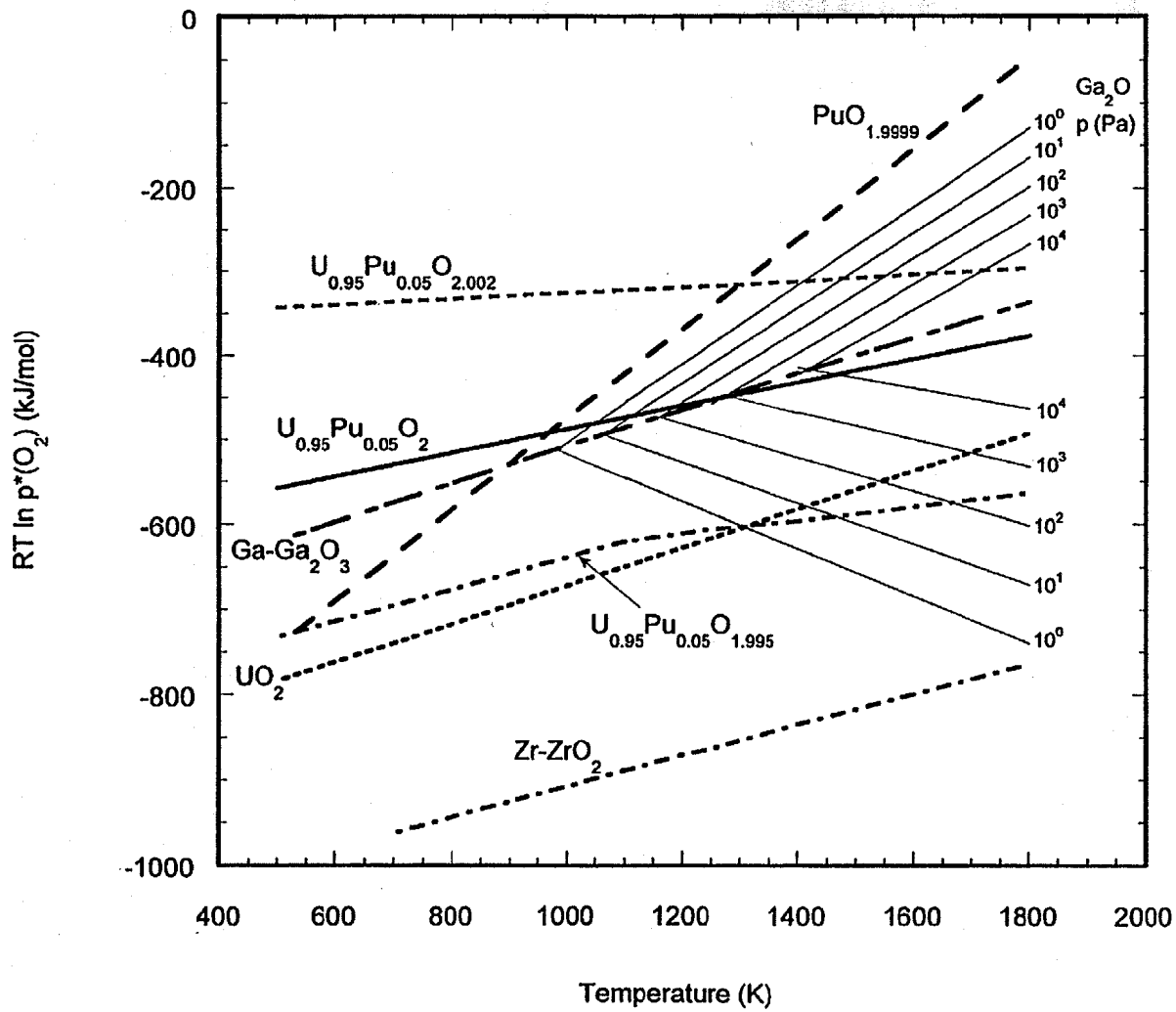

Fig. 36. Phase stability diagram for oxides of interest.[1]

6. CONCLUSIONS

6.1 PHASE I

Corrosion testing revealed that liquid gallium reacts with Zircaloy to form an IC of the form Zr_xGa_y. The extent of reaction is a function of temperature, but more importantly, is strongly dependent on the amount of gallium involved. Although distortion of some Zircaloys can be a by-product of ICF at >300°C, distortion in susceptible materials at 500°C did not occur at ratios of weight of gallium to surface area of Zircaloy that were 10^4 to 10^5 higher than those expected with WG-MOX fuel in an LWR fuel pin. Mechanical property testing after corrosion exposure to form a thin IC layer on the gage section of Zircaloy specimens further confirmed that there should be little effect of small quantities of gallium in MOX fuel on the Zircaloy cladding.

No localized corrosion effects were found. In the corrosion tests (up to 500°C), there was no evidence of grain boundary attack in addition to ICF. In the LME tests at 30 and 100°C, there was no change in the tensile properties when Zircaloy was tested in liquid gallium and the fracture remained ductile.

6.2 PHASE II

Results of testing in Ga_2O_3 or Ce_2O_3-Ga_2O_3 mixtures did not indicate any significant effects at 300°C. At 500°C, an oxide layer formed on the Zircaloy and room-temperature tensile tests for two of the materials showed a loss in strength with a corresponding increase in ductility. The oxide layer also formed during exposure of Zircaloy to several other oxide powders, making it uncertain whether any of the observed mechanical effects are related to the presence of gallium.

At 700°C, which is considerably above LWR operating temperatures, there was evidence of reduction of Ga_2O_3 by Zircaloy and formation of a gallium-rich corrosion product below the ubiquitous oxide layer. However, this gallium-rich zone was not confirmed in tests with <100% Ga_2O_3.

Based on the results obtained, it does not appear that 1 to 10 ppm gallium in MOX fuel will have any measurable effect on the properties of Zircaloy cladding.

7. REFERENCES

1. D. F. Wilson et al., *Potential Effects of Gallium on Cladding Materials*, ORNL/TM-13504, Lockheed Martin Energy Research Corp., Oak Ridge Natl. Lab., 1997.

2. D. F. Wilson et al., *Interactions of Zircaloy Cladding with Gallium 1997 Status,* ORNL/TM-13505, Lockheed Martin Energy Research Corp., Oak Ridge Natl. Lab., 1997.

3. D. F. Wilson et al., *Interactions of Zircaloy Cladding with Gallium: 1998 Midyear Status,* ORNL/TM-13625, Lockheed Martin Energy Research Corp., Oak Ridge Natl. Lab., 1998.

4. T. B. Massalski, ed., *Binary Alloy Phase Diagrams* 2, ASM International, Metals Park, Ohio, 1990, p. 1880.

5. H. S. Rosenbaum, *Electrochemical Technology* **4**, 153 (1966).

6. H. S. Rosenbaum, J. H. Davies, and J. Q. Pon, *EURAEC Report*, GEAP 5100-5105, 1966.

7. W. T. Grubb, "Cadmium Embrittlement of Zircaloy-2 and Certain Other Metals and Alloys," pp. 473–484 in *Embrittlement by Liquid and Solid Metals*, ed. M. H. Kamdar, The Metallurgical Society of AIME, Warrendale, Penn., 1984.

8. R. P. Gangloff, "Solid Cadmium Embrittlement of Textured Zircaloy-2," pp. 485–505 in *Embrittlement by Liquid and Solid Metals*, ed. M. H. Kamdar, The Metallurgical Society of AIME, Warrendale, Penn., 1984.

9. B. Cox, *Environmentally Induced Cracking of Zirconium Alloys: II-Liquid Metal Embrittlement*, AECL-3612, Atomic Energy of Canada, Ontario, Canada, 1970.

10. T. Watanabe, S. Shima, and S. Karashima, "Liquid Metal Gallium Induced Intergranular Fracture of Aluminum Bicrystals," pp. 173–182 in *Embrittlement by Liquid and Solid Metals*, ed. M. H. Kamdar, The Metallurgical Society of AIME, Warrendale, Penn., 1984.

11. H. Ichinose and T. Takashima, "Grain Boundary Diffusion and Static Fatigue of Aluminum by Liquid Gallium," pp. 197–210 in *Embrittlement by Liquid and Solid Metals*, ed. M. H. Kamdar, The Metallurgical Society of AIME, Warrendale, Penn., 1984.

12. W. T. Grubb and M. H. Morgan III, "A Survey of Chemical Environments for Activity in the Embrittlement of Zircaloy-2," pp. 145–154 in *Proceedings of the Fourth International Conference: Zirconium in the Nuclear Industry*, ASTM STP 681, American Society for Testing and Materials, Philadelphia, 1979.

13. H. R. Trellue et al., *Nuclear Fuels Technologies Fiscal Year 1997 Research and Development Test Results*, LA-UR-97-4423, Univ. of Calif., Los Alamos Natl. Lab., 1997.

14. A. R. C. Westwood and R. M. Latanision, "Adsorption-Induced Embrittlement by Liquid Metals," pp. 405–415 in *Proceedings of Corrosion by Liquid Metals*, ed. J. E. Draly and J. R. Weeks, The Metallurgical Society of AIME, Philadelphia, 1969.

15. N. S. Stoloff and T. L. Johnson, *Acta Met.* **11**, 251 (1963).

16. V. V. Popovich, *Phys. Chem. Mech. Materials*, USSR 5 (1979).

17. S. P. Lynch, *Acta Met.* **36**, 2639 (1988).

18. W. Rostoker, J. M. McCaughey and H. Markus, **Embrittlement by Liquid Metals**, Reinhold, New York, New York, 1960.

19. V. I. Likhtman, E. D. Shchukin, and P. A. Rebinder, **Physicochemical Mechanics of Metals**, Academy of Sciences, USSR 1962.

20. N. B. Pilling and R. E. Bedworth, *J. Inst. Metals,* **29**, 529 (1923).

APPENDIX

The following tables summarize the status of the work performed. Nonvendor-supplied materials are listed with their trade names. Vendor-supplied materials are listed with generic names.

Table A.1. Supplemental compatibility tests of zirconium/Zircaloy with gallium or Ga_2O_3 in support of test design

Material	Test environment	Temp. (°C)	Time (h)	Comments
Zr	Ga	400	100	Intermetallic compound formation (ICF)
Zr	Ga	600	134	ICF
Zircaloy-2	Ga	400	100	ICF
Zircaloy-2	Ga	600	100	ICF
Zircaloy-2	Ga_2O_3	400	200	Thin ZrO_2 layer visible at 1000X
Zircaloy-2	Ga_2O_3	600	200	Slightly thicker ZrO_2 layer visible at 1000X
Zircaloy-2	Ga_2O_3	500	672	ZrO_2 layer plus Ga within alloy
Zircaloy-2	Ga_2O_3	500	2016	ZrO_2 layer plus Ga within alloy; no change in thickness (compared with 4 weeks)
Zircaloy-4	Ga_2O_3	700	672	Much thicker ZrO_2 layer (compared with 500°C), plus ICF below oxide; cracks in ZrO_2
Zircaloy-4	Ga_2O_3	700	2016	4-mil ZrO_2 layer plus 3 mils of ICF below oxide
Zircaloy-B (vendor)	Ga	500	200	Electron beam welding (EBW) (vacuum); ICF; very slight distortion
Zircaloy-C (vendor)	Ga	500	200	EBW (vacuum); ICF; distortion
Zircaloy-B (vendor)	Ga	500	200	Thin end cap (0.50 in.); ICF; very slight distortion
Zircaloy-B (vendor)	Ga	500	200	Thick end cap (0.2 in.) with circumferential laser beam welding (LBW) of end cap to seal crevice; ICF; distortion
Zircaloy-C (vendor)	Ga	500	200	Thin end cap; ICF; distortion
Zircaloy-C (vendor)	Ga	500	200	Thick end cap with LBW; ICF; distortion
Zircaloy-C (vendor)	Ga	500	200	~650 ppm Ga in ZrO_2 powder
Zircaloy-C (vendor)	Ga	500	200	~650 ppm Ga at bottom of capsule covered with ZrO_2 powder
Zircaloy-4	Ga_2O_3	700	672	~1800 ppm Ga_2O_3 blended with ZrO_2; interaction to <0.5 mil
Zircaloy-C (vendor)	ZrO_2	500	200	ZrO_2 as surrogate

Table A.1. Supplemental compatibility tests of zirconium/Zircaloy with gallium or Ga_2O_3 in support of test design

Material	Test environment	Temp. (°C)	Time (h)	Comments
Zircaloy-C (vendor)	CaO	500	200	CaO as surrogate
Zircaloy-B (vendor)	Ce_2O_3	500	200	Ce_2O_3 as surrogate
Zircaloy-B (vendor)	Ga	500	200	3 g Ga; evaluation of tungsten (W) insert geometry for liquid metal embrittlement (LME) & corrosion-mechanical (C-M) tests
Zircaloy-C (vendor)	Ga	500	200	3 g Ga; evaluation of W insert geometry for LME & C-M tests
Zircaloy-C (vendor)	—			No insert; evaluation of specimen geometry for LME & C-M tests
Zircaloy-C (vendor)	Ga			Large insert; evaluation of W insert for LME & C-M tests
Zircaloy-C (vendor)	Ga			No insert; evaluation of specimen geometry for LME & C-M tests
Zircaloy-C (vendor)	Ga			Small insert; evaluation of W insert for LME and C-M tests
Zircaloy-C (vendor)	Ga	300	200	Determine acceptable, f(T), (no swelling & very thin corrosion layer) corrosion conditions for C-M tests
Zircaloy-C (vendor)	Ga	400	200	Determine acceptable, f(T), (no swelling & very thin corrosion layer) corrosion conditions for C-M tests
Zircaloy-C (vendor)	Ga	350	200	Determine acceptable, f(T), (no swelling & very thin corrosion layer) corrosion conditions for C-M tests
Zircaloy-B (vendor)	Ga	300	100	Determine acceptable, f(t), (no swelling & and very thin corrosion layer) corrosion conditions for C-M tests
Zircaloy-B (vendor)	Ga	300	25	Determine acceptable, f(t), (no swelling & very thin corrosion layer) corrosion conditions for C-M tests
Zircaloy-B (vendor)	Ga	300	50	Determine acceptable, f(t), (no swelling & very thin corrosion layer) corrosion conditions for C-M tests
Zircaloy-A (vendor)	Ga	500	200	Comparison of distortion, f(material)
Zircaloy-B (vendor)	Ga	500	200	Comparison of distortion, f(material)
Zircaloy-C (vendor)	Ga	500	200	Comparison of distortion, f(material)
Zircaloy-A (vendor)	Ga/Cd	500	200	Comparison of distortion, f(material)
Zircaloy-B (vendor)	Ga/Cd	500	200	Comparison of distortion, f(material)
Zircaloy-C (vendor)	Ga/Cd	500	200	Comparison of distortion, f(material)
Zircaloy-A (vendor)	Ga	500	200	25 mg Ga; demonstrate amount of attack with decreasing Ga mass

Table A.1. Supplemental compatibility tests of zirconium/Zircaloy with gallium or Ga_2O_3 in support of test design

Material	Test environment	Temp. (°C)	Time (h)	Comments
Zircaloy-B (vendor)	Ga	500	200	25 mg Ga; demonstrate amount of attack with decreasing Ga mass
Zircaloy-C (vendor)	Ga	500	200	25 mg Ga; demonstrate amount of attack with decreasing Ga mass
Zircaloy-A (vendor)	Ga	500	200	2.5 mg Ga; demonstrate amount of attack with decreasing Ga mass
Zircaloy-B (vendor)	Ga	500	200	2.5 mg Ga; demonstrate amount of attack with decreasing Ga mass
Zircaloy-C (vendor)	Ga	500	200	2.5 mg Ga; demonstrate amount of attack with decreasing Ga mass
Zircaloy-A (vendor)	Ga	500	200	0.25 mg Ga; demonstrate amount of attack with decreasing Ga mass
Zircaloy-B (vendor)	Ga	500	200	0.25 mg Ga; demonstrate amount of attack with decreasing Ga mass
Zircaloy-C (vendor)	Ga	500	200	0.25 mg Ga; demonstrate amount of attack with decreasing Ga mass

Table A.2. Status of corrosion tests of Zircaloy with gallium metal

Material	Time (h)	Temperature (°C)				Comment
		30	100	500	500[a]	
Zircaloy-A (vendor)	200			✔[b]	✔	No attack at 30 or 100°C; Intermetallic compound formation (ICF) at 500°C
	700	✔	✔	✔	✔	
Zircaloy-B (vendor)	200			✔	✔	ICF; dimensional distortion
	700	✔	✔	✔	✔	No attack at 30 or 100°C; ICF at 500°C but no increase over 200 h; dimensional distortion
Zircaloy-C (vendor)	200			✔	✔	ICF; dimensional distortion
	700	✔	✔	✔	✔	No attack at 30 or 100°C; ICF at 500°C but no increase over 200 h; dimensional distortion at 500°C

[a] With cadmium.
[b] ✔ — Completed test.

Table A.3. Status of corrosion tests of Zircaloy with Ga_2O_3

Materials	Ga_2O_3 (wt %)	Time (weeks)	Temperature (°C) 300	500	700	Comment
Zircaloy-A (vendor)	100	6	✔[a]	✔	✔	
	100	12	✔	✔	✔	
	1.0	6	✔	✔	✔	
	0.2	6	✔	✔	✔	
	0.1	6	✔	✔	✔	
Zircaloy-B (vendor)	100	6	✔	✔	✔	No interaction at 300°C; ZrO_2 at 500 and 700°C; intermetallic compound formation (ICF) at 700°C
	100	12	✔	✔	✔	Same as for 6 weeks except greater depth of interaction at 700°C
	1.0	6	✔	✔	✔	
	0.2	6	✔	✔	✔	
	0.1	6	✔	✔	✔	
Zircaloy-C (vendor)	100	6	✔	✔	✔	No interaction at 300°C; ZrO_2 at 500 and 700°C; ICF at 700°C
	100	12	✔	✔	✔	Same as for 6 weeks except greater depth of interaction at 700°C
	1.0	6	✔	✔	✔	
	0.2	6	✔	✔	✔	
	0.1	6	✔	✔	✔	

[a] ✔ — Completed.

Table A.4. Status of mechanical tests of Zircaloy with gallium metal

Material	Type	Temperature (°C) 30	100	300	300[a]	Comment
Zircaloy-A (vendor)	LME[b]	✔[c]	✔			
	CM[d]			✔	x[e]	
Zircaloy-B (vendor)	LME	✔	✔			
	CM			✔	x	
Zircaloy-C (vendor)	LME	✔	✔			
	CM			✔	x	Fracture surface exhibited nonductile features

[a] With cadmium.
[b] LME — Constant extension rate tensile (CERT) test at temperature (triplicate tests).
[c] ✔ — Completed test.
[d] CM — CERT test at room temperature after 200 h at temperature (triplicate tests).
[e] x — Cancelled.

Table A.5. Status of room-temperature, corrosion-mechanical[a] tests of Zircaloy with Ga_2O_3

Materials	Ga_2O_3 (wt %)	Temperature (°C) 300	500	700	Comment
Zircaloy-A (vendor)	100	✔[b]	✔	x[c]	
	1.0	✔	✔	x	
	0.2	✔	✔	x	
	0.1	✔	✔	x	
	0	✔	✔	x	
	empty	✔	✔	x	
Zircaloy-B (vendor)	100	✔	✔	x	
	1.0	✔	✔	x	
	0.2	✔	✔	x	
	0.1	✔	✔	x	
	0	✔	✔	x	
	empty	✔	✔	x	
Zircaloy-C (vendor)	100	✔	✔	x	
	1.0	✔	✔	x	
	0.2	✔	✔	x	
	0.1	✔	✔	x	
	0	✔	✔	x	
	empty	✔	✔	x	

[a] Constant extension rate tensile test at room temperature after 6 weeks at temperature (triplicate tests).
[b] ✔ — Completed.
[c] x — Cancelled.

Table A.6. Status of high-temperature tensile, corrosion-mechanical[a] tests of Zircaloy with Ga_2O_3

Materials	Ga_2O_3 (wt %)	Temperature (°C) 300	500	Comment
Zircaloy-A (vendor)	100	✔[b]	✔	
	1.0	x[c]	x	
	0.2	x	x	
	0.1	✔	✔	
	0	x	x	
	empty	✔	✔	
Zircaloy-B (vendor)	100	x	x	
	1.0	x	x	
	0.2	x	x	
	0.1	x	x	
	0	x	x	
	empty	x	x	
Zircaloy-C (vendor)	100	✔	✔	
	1.0	x	x	
	0.2	x	x	
	0.1	✔	✔	
	0	x	x	
	empty	✔	✔	

[a] Constant extension rate tensile test at temperature after 6 weeks at temperature (triplicate tests).
[b] ✔ — Completed duplicate tests.
[c] x — Cancelled.

INTERNAL DISTRIBUTION

1. C. A. Baldwin
2. E. C. Beahm
3. T. M. Besmann
4. B. B. Bevard
5. R. A. Bradley
6. S. L. Byerly
7. J. J. Carbajo
8. E. D. Collins
9. B. S. Cowell
10. D. F. Craig
11. J. H. DeVan
12–14. J. R. DiStefano
15. E. E. Duncan
16. E. C. Fox
17. U. Gat
18. R. G. Gilliland
19. S. R. Greene
20. H. W. Hayden
21. S. A. Hodge
22. J. A. Horak
23. L. L. Horton
24. J. R. Keiser
25–27. J. F. King
28–30. E. T. Manneschmidt
31. S. R. Martin, Jr., DOE/ORO
32. G. T. Mays
33. G. E. Michaels
34. R. N. Morris
35. N. H. Packan
36. S. J. Pawel
37. R. T. Primm, III
38. D. G. O'Connor
39. L. J. Ott
40. R. R. Rahn
41. J. D. Sease
42. C. C. Southmayd
43. D. J. Spellman
44–46. J. P. Strizak
47. K. R. Thoms
48. D. L. Williams, Jr.
49–58. D. F. Wilson
59. B. A. Worley
60. Central Research Library
61. ORNL Laboratory Records–RC
62–63. ORNL Laboratory Records–OSTI
64. FMDP Library

EXTERNAL DISTRIBUTION

65. M. L. Adams, Amarillo National Resource Center for Plutonium, Department of Nuclear Engineering, Texas A&M University, College Station, TX 77843-3133

66. D. Alberstein, Los Alamos National Laboratory, P. O. Box 1663, MS-K551, Los Alamos, NM 87545

67. J. F. Baker, U.S. Department of Energy, MD-1, Forrestal Building, 1000 Independence Avenue SW, Washington, DC 20585

68. T. Barr, U.S. Department of Energy, EPG, Argonne National Laboratory, 9800 South Cass Avenue, Argonne, IL 60439

69. F. R. Best, Amarillo National Resource Center for Plutonium, Associate Professor, Department of Nuclear Engineering, Texas A&M University, College Station, TX 77843-3133

70. J. J. Buksa, Los Alamos National Laboratory, P. O. Box 1663, MS-F628, Los Alamos, NM 87545

71. D. P. Butt, Los Alamos National Laboratory, P. O. Box 1663, MS-G755, Los Alamos, NM 87545

72. H. R. Canter, U.S. Department of Energy, MD-1, Forrestal Building, 1000 Independence Avenue SW, Washington, DC 20585

73. A. I. Cygelman, U.S. Department of Energy, MD-3, Forrestal Building, 1000 Independence Avenue SW, Washington, DC 20585

74. T. H. Gould, Jr., Lawrence Livermore National Laboratory, P. O. Box 808, MS-L186, Livermore, CA 94551

75. R. J. Hanrahan Jr., Los Alamos National Laboratory, P. O. Box 1663, MS-G770, Los Alamos, NM 87545

76. R. R. Hart, Amarillo National Resource Center for Plutonium, Professor, Department of Nuclear Engineering, Texas A&M University, College Station, TX 77843-3133

77. H. C. Irwin, Sandia National Laboratories, P. O. Box 969, MS-9015, Livermore, CA 94551

78. S. O'Kelly, Amarillo National Resource Center for Plutonium, Assistant Director, Nuclear Science Center, Texas A&M University, College Station, TX 77843-3575

79. A. D. Neuman, Los Alamos National Laboratory, P. O. Box 1663, MS-E502, Los Alamos, NM 87545

80. D. J. Nulton, U.S. Department of Energy, MD-4, Forrestal Building, Room 6G-050, 1000 Independence Avenue SW, Washington, DC 20585

80–81. C. J. Paone, General Electric Company, P. O. Box 780, M/C A16, 3901 Castle Hayne Road, Wilmington, NC 28402

82. D. Peko, U.S. Department of Energy, MD-3, Forrestal Building, Room 6G-050, 1000 Independence Avenue SW, Washington, DC 20585

83–87. P. T. Rhoads, U.S. Department of Energy, MD-3, Forrestal Building, Room 6G-050, 1000 Independence Avenue SW, Washington, DC 20585

88. P. L. Rittenhouse, 346 Myers Road, Kingston, TN 37763

89–90. S. Ritterbusch, ABB Combustion Engineering Nuclear Systems, 2000 Day Hill Road, Windsor, CT 06095-0500

91. J. M. Ryskamp, Idaho National Engineering and Environmental Laboratory, P. O. Box 1625, Idaho Falls, ID 83415-3885

92. G. B. Stevenson, U.S. Department of Energy, MD-4, Forrestal Building, Room 6G-050, 1000 Independence Avenue SW, Washington, DC 20585

93. J. H. Thompson, U.S. Department of Energy, MD-4, Forrestal Building, Room 6G-050, 1000 Independence Avenue SW, Washington, DC 20585

94–95. M. Travis, Westinghouse Electric Corporation, P. O. Box 355, Pittsburgh, PA 15230

96. S. S. Voss, Los Alamos National Laboratory, P.O. Box 1663, MS-F628, Los Alamos, NM 87545